Received: 1 July 2021 | Revised: 20 April 2022 | Accepted: 17 May 2022

DOI: 10.1002/ajpa.24570

RESEARCH ARTICLE

AMERICAN JOURNAL OF BIOLOGICAL ANTHROPOLOGY
The Official Journal of the American Association of Biological Anthropologists
WILEY

New hominin dental remains from the Drimolen Main Quarry, South Africa (1999–2008)

Angeline B. Leece[1] | Jesse M. Martin[1] | Andy I. R. Herries[1,2] | Alessandro Riga[3] | Colin G. Menter[3] | Jacopo Moggi-Cecchi[3]

[1]Palaeoscience Labs, Department of Archaeology and History, La Trobe University, Melbourne Campus, Bundoora, Victoria, Australia

[2]Palaeo Research Institute, Humanities Research Village, University of Johannesburg, Auckland Park, South Africa

[3]Department of Biology, University of Florence, Florence, Italy

Correspondence
Jacopo Moggi-Cecchi, Department of Biology, University of Florence, Via del Proconsolo, 12, 50122 Florence, Italy.
Email: iacopo.moggicecchi@unifi.it

Funding information
Australian Archaeological Association, Grant/Award Number: SRGS 2014; Australian Research Council, Grant/Award Numbers: Discovery grant DP170100056, Future Fellowship grant FT120100399; Italian Ministry of Foreign Affairs; La Trobe University, Grant/Award Number: IRGS

Abstract

Objectives: Twenty-four dental specimens from the Drimolen Main Quarry (DMQ) are described. This increases the number of DMQ *Paranthropus robustus* specimens from 48 to 63 and DMQ *Homo* specimens from 8 to 12. This allows reassessment of the proposed differences between the DMQ *P. robustus* assemblage and that of Swartkrans. Analysis conducted assesses intraspecific and inter-locality variation.

Materials and Methods: We examined the *P. robustus* and early *Homo* assemblages from South Africa. Morphology was observed using a hand lens and a binocular microscope. Mesiodistal and buccolingual measurements were taken using plastic-tipped calipers. Summary statistics were generated and patterns of variability in *P. robustus* were assessed through box plots and Mann–Whitney *U* tests.

Results: Comparison between the expanded DMQ and Swartkrans *P. robustus* assemblages demonstrates overlap in size. Ten dental variables show statistically significant differences.

Discussion: The expanded *P. robustus* sample allowed us to re-examine previous analyses of differences in tooth size between the samples. While analyses presented here show a high degree of overlap in the MD and BL dimensions of the two assemblages, significant differences were found in the mean values of these variables in the postcanine maxillary teeth—consistent with previous analyses. Two current hypotheses may explain this pattern: 1) dental size increase through the *P. robustus* lineage or 2) different sample composition between the two sites. Small sample sizes for all permanent dental classes in the DMQ assemblage represents a limitation on this analysis and interpretations thereof. Any addition to the DMQ or the Swartkrans samples may alter these results.

KEYWORDS
dentition, Drimolen Main Quarry, early *Homo*, paleocave, *Paranthropus robustus*, Swartkrans

1 | INTRODUCTION

The hominin-bearing paleocave system of Drimolen is located within the Fossil Hominid Sites of South Africa UNESCO world heritage area in the Gauteng province, South Africa (also known as the Cradle of Humankind; Figure 1). Discovered in 1992 (Keyser et al., 2000), the site is approximately 6 km north east of the hominin bearing paleocaves of Sterkfontein and Swartkrans (Herries et al., 2020; Keyser et al., 2000). Like other sites, such as Kromdraai, Sterkfontein, and Swartkrans, Drimolen is now known to contain at least two separate fossil paleocave deposits (Rovinsky et al., 2015). The older of these, the Drimolen Makondo (DMK), is dated to ~2.61 Ma, has only been excavated since 2014, and has not yielded any hominins (Herries et al., 2018; Rovinsky et al., 2015). The younger, classic site discovered in 1992 is now referred to as the Drimolen Main Quarry (DMQ) and dates to between ~2.04 and 1.95 Ma (Herries et al., 2020). The two deposits are around 50 m apart and there is currently no evidence that they were stratigraphically connected (Murszewski et al., 2020). Excavations conducted at DMQ since initial discovery have produced a large faunal assemblage (Adams et al., 2016) as well as hominin specimens representing *Paranthropus robustus*, *Homo* aff. *erectus*, and early *Homo* sp. (Herries et al., 2020; Keyser et al., 2000; Martin et al., 2021; Moggi-Cecchi et al., 2010). The majority of the hominin assemblage is represented by isolated dental elements, with notable exceptions including the nearly complete *P. robustus* skull, DNH 7 (Keyser, 2000; Rak et al., 2021), the DNH 20, DNH 152, and DNH 155 *P. robustus* crania (Herries et al., 2020; Keyser et al., 2000; Martin et al., 2021), and the DNH 134 neurocranium attributed to *Homo* aff. *erectus* (Herries et al., 2020). Detailed descriptions of most of the dental specimens listed by Keyser et al. (2000) and excavated prior to 1999 have been previously published (Keyser, 2000, Schwartz & Schwartz & Tattersall, 2005, Moggi-Cecchi et al., 2010; Rak et al., 2021), along with a number of recent discoveries since 2018 that are associated with *P. robustus* crania (Herries et al., 2020; Martin et al., 2021). Here, dental remains recovered between 1999 and 2008 are described.

As the DMQ and Swartkrans assemblages make up the majority of the *P. robustus* fossil record, Moggi-Cecchi et al. (2010) performed a statistical comparison of the mesiodistal (MD) and buccolingual (BL) measurements of these two samples. That analysis found the DMQ *P. robustus* dental sample to be characterized by overall smaller permanent and deciduous teeth than the Swartkrans sample (and in some cases also smaller than the limited Kromdraai B sample; Braga, Dumoncel, et al., 2016), as well as a greater size range, described by the coefficient of variation of the two groups. Despite the limited samples sizes available, Moggi-Cecchi et al. (2010, p. 404) presented "the possibility that some kind of selective agent and/or taphonomic bias has produced a differential accumulation of a relatively larger number of small individuals in the DMQ sample or of a relatively larger number of large individuals in the Swartkrans sample" and suggested that "the Swartkrans sample, mostly resulting from an accumulation due to carnivore activity, seems to display a relative abundance of male specimens (at least among the well preserved skulls)." The issue of dental size variability and distribution between these samples must be investigated to gain information on the biology of the two populations, and, more broadly, of the species *P. robustus*.

A further 24 dental specimens are presented in this paper including morphological descriptions, taxonomic attributions, standard dental measurements (MD and BL diameters) together with a basic statistical analysis of the expanded Drimolen dental sample. The addition of these 24 specimens, as well as Swartkrans specimens that have been published since Moggi-Cecchi et al.'s (2010) analyses (Pickering et al., 2012; Pickering et al., 2016; Sutton et al., 2009), allows for a reassessment of previous results.

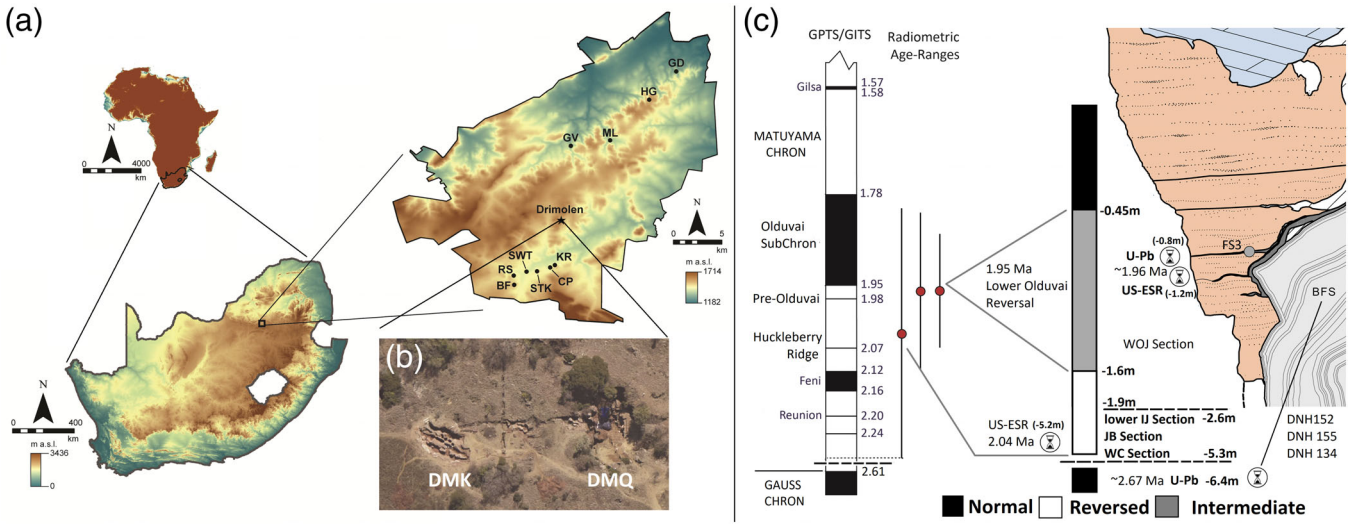

FIGURE 1 (a) Location of Drimolen compared to other fossil sites in the Cradle of Humankind, South Africa; (b) the relationship between the older ~2.61 Ma Drimolen Makondo (DMK) and younger hominin bearing Drimolen Main Quarry (DMQ) paleocaves; (c) the dating of the DMQ deposits (Depth shown in meters). IJ, Italian Job Section; JB, Jangi Buttress Section; WC, Warthog Cave section; WOJ, Walls of Jericho Section

A broader analysis has been conducted here with the aim of assessing variation at Drimolen and Swartkrans, both internally and between the two localities.

Previous analysis (Moggi-Cecchi et al., 2010) indicated the occurrence of an undetermined species of the genus *Homo* at the DMQ site, represented by 9 specimens that increase the relatively small sample of Early Pleistocene *Homo* from South African sites. Fossils attributed to early *Homo* have also been documented from a number of sites. At Swartkrans Members 1 and 2 (see Grine, 2005 and Grine et al., 2009 for a review plus Pickering et al., 2012), craniodental specimens include the crania SK 847, SK 27, the mandibles SK 15, SK 45, and SKX 21204, plus a number of isolated teeth. At Sterkfontein (Member 5) specimens include the cranium StW 53, the mandible StW 80, (and possibly StW 151), together with several isolated teeth (Grine et al., 2009; Kuman & Clarke, 2000). In addition two teeth reworked from Member 5 were recovered from the Sterkfontein Lincoln Cave deposits (Reynolds et al., 2007) and another from the Milner Hall (StW 669) (Stratford et al., 2016). Evidence of early *Homo* at Kromdraai (represented by the specimen KB 5223) (Braga & Thackeray, 2003) is disputed (Grine et al., 2009). Another specimen has been recovered from the open air site of Cornelia-Uitzoek in the Free State; it is the youngest specimen attributed to early *Homo* and the oldest hominin outside of the restricted paleocaves of the Malmani dolomite (Brink et al., 2012). Potential early *Homo* isolated partial molars have also been recovered from the sites of Gondolin and Haasgat (Leece et al., 2016; Menter et al., 1999).

The systematics of the early *Homo* specimens recovered at South African sites is still a matter of debate. Even in the case of more complete specimens (e.g. SK 847, SK 15, and Stw 53) no agreement has been reached among researchers on their attribution at a specific level. Suggestions include attributing all the South African early *Homo* fossils to a single species (*Homo habilis*, *Homo ergaster* or to new species not sampled in East Africa), or to different species (Zanolli et al., 2018; see also Grine et al., 2009 for a review). The exception to this is the DNH 134 cranium from DMQ that represents possibly the earliest specimen of *Homo* from South Africa (SKX 21204 from Swartkrans Member 1 Lower Bank could be older; see discussion), and the only South African specimen that can be confidently attributed to *H.* aff. *Erectus* (Herries et al., 2020). However, the DNH 134 cranium does not preserve any teeth, so direct comparison to the relatively larger sample of *Homo* dentition from South Africa is not possible.

2 | SITE AND SAMPLE PROVENIENCE

2.1 | Site and stratigraphy

DMQ consists of a large single paleocavern that has been quite extensively mined for its speleothem (stalagmites and flowstones) in the late 19th and early 20th century. Unlike sites such as Sterkfontein and Swartkrans, DMQ has a relatively simple depositional sequence, but with distinct lateral variation of sedimentological facies (Herries et al., 2020; Keyser et al., 2000). The macrofossil remains, including the hominins, have been recovered from three major types of deposit (Adams et al., 2016; Herries et al., 2020; Keyser, 2000; Keyser et al., 2000; Martin et al., 2021; Moggi-Cecchi et al., 2010). Some material, such as DNH 155, DNH 152 and DNH 134, have been recovered from in situ breccia remnants of a large talus cone formed in the western central portion of the DMQ paleocavern (Warthog Cave (WC), Jangi Buttress (JB), and lower Italian Job (IJ) sections in Figure 1c)., or from recently decalcified parts of this talus cone breccia (Herries et al., 2020). Fossils such as DNH 7 have been recovered from well-defined ex-situ collapse breccia and its decalcified components within the Central Excavation Area of the site (Herries et al., 2019, 2020; Keyser et al., 2000). Other fossils have been recovered from lime-miners rubble that dominates the eastern part of DMQ.

The DMQ stratigraphy consists of a basal flowstone overlain in the center of the paleocavern by the breccia of the talus cone that formed from a central vertical entrance. The deposition of the basal flowstone ended between 2.8 and 2.6 Ma based on uranium-lead (U–Pb) dating (Herries et al., 2020). A uranium series-electron spin resonance (US-ESR) age of 2.04 ± 0.24 Ma from the Jangi Buttress (Figure 1c) indicates that fossil and sediment infill began at least 400,000 years after the formation of the basal flowstone (Herries et al., 2020). Flooding of the cave then winnowed fine-grained sediments from the matrix of the central debris pile breccia and redeposited them against the walls of the cave, forming laminated sandstone and siltstone deposits, with the occasional interstratified flowstone. The sandstone and siltstone deposits at DMQ (Figure 1c) record a reversed magnetic polarity at the base of the sequence followed by a long period of intermediate polarity and then a short period of normal polarity close to the cave roof (Herries et al., 2020). This magnetic reversal has been identified as the base of the Olduvai SubChron at 1.95 Ma based on the U–Pb dating of a flowstone that formed during the intermediate polarity transition to 1.96 ± 0.11 Ma and a US-ESR age of 1.97 ± 0.15 Ma just below this flowstone (Herries et al., 2020; Figure 1c). As such, the majority of in situ fossils recovered from the DMQ excavations can be confidently dated to between 1.95 Ma and ~2.04 Ma (Not older than 2.28 Ma; Herries et al., 2020). The high-resolution nature of the reversal indicates that the top 2 m of the deposits formed around and during the reversal itself at ~1.95 Ma (Herries et al., 2020). While a slightly younger US-ESR age of 1.712 ± 0.538 Ma came from a tooth in the decalcified DNH 7 yielding collapsed breccia block, this age still overlaps with the others within error (2.35–1.174 Ma). The high uncertainty in the age is due to the effects of decalcification on these deposits, making dosimetry far more complex (Herries et al., 2019, 2020). Similar underestimations in age on teeth from decalcified deposits have been noted when comparing ESR ages on teeth from calcified and decalcified deposits at Sterkfontein (Herries & Shaw, 2011). Given the understanding of the stratigraphy and chronology of the site there is no reason to suppose that all this fossil material recovered from ex situ contexts does not

date to between ~2.04 and 1.95 Ma like the in-situ deposits (Herries et al., 2020).

2.2 | Hominin sample

The majority of the DMQ hominin assemblage is represented by isolated dental elements or teeth in maxillary or mandibular fragments. This may relate to the greater survival of enamel in sediments that have undergone significant decalcification, rather than a true representation of the skeletal elements originally deposited in the cave. The DNH 7 cranium was notably recovered decalcifying out of solid, but ex-situ collapsed breccia (Keyser et al., 2000). The DNH 134, 155, and 152 crania were all found within a mixture of decalcified and still lightly calcified breccia within a few cm of well indurated in situ breccia (Herries et al., 2020; Martin et al., 2021). However, the preservation bias may also relate to the nature of the deposition of the fossils at the site, with fossils having been washed down a vertical entrance cave shaft (Herries et al., 2020). The occurrence of more complete crania and post-cranial elements alongside isolated teeth may suggest a mixture of taphonomic processes occurring at the site, or change through time as the morphology of the cave and cavern changes. However, despite there being a range of larger carnivores represented at DMQ (Adams et al., 2016) there is no direct evidence that carnivores introduced hominin remains to the cave. This contrasts with the Swartkrans assemblage where direct evidence of hominin and carnivore interaction exists (Brain, 1981, 1993).

3 | DESCRIPTIONS

Qualitative analysis of the new DMQ dental specimens was conducted in the form of anatomical descriptions. All specimens were examined using both a hand lens with 10× and 20× magnification and a low-powered binocular microscope. Distinct morphological features reported by Moggi-Cecchi et al. (2010) as well as earlier studies of South African *P. robustus* and early *Homo* (Robinson, 1953; Robinson, 1956; Tobias, 1965, 1967, 1991; Clarke, 1977; Howell, 1978; Grine, 1984, 1989, 2005; Grine & Strait, 1994) were utilized for the purposes of assessing classic *P. robustus* and early *Homo* dental morphological traits. For those tooth classes where no early *Homo* specimens are available in the South African fossil record, traits refer to "non-robust" specimens. Taking into account the dental elements recognized, for each tooth class the following features have been assessed:

3.1 | Maxillary deciduous teeth

3.1.1 | Incisors

Paranthropus: crown short inciso-cervically and broad at the cervix.
Homo: crown tall inciso-cervically and slender.

3.1.2 | Canines

Paranthropus: buccal face of the crown slightly convex in mesiodistal direction; mesiodistal dimension reduced.
Homo: buccal face of the crown markedly convex in mesiodistal direction; mesiodistal dimension elongated.

3.1.3 | Molars

Paranthropus: lingual aspect of the protocone is strongly inflated; paracone equal in size to metacone; *tuberculum molare* small or absent; distal marginal ridge thick and high; buccal groove absent; mesio-buccal groove weak.
Homo: lingual aspect of the protocone is moderately beveled; paracone larger than metacone; *tuberculum molare* moderate to well developed; distal marginal ridge narrow and moderately high; buccal groove V shaped; mesio-buccal groove marked.

3.2 | Mandibular deciduous teeth

3.2.1 | Incisors

Paranthropus: crown dimensions small.
Homo: crown dimensions larger.

3.3 | Maxillary permanent teeth

3.3.1 | Incisors

Paranthropus: crown short inciso-cervically and broad; crown mesiodistally reduced.
Homo: crown tall inciso-cervically and slender; crown mesiodistally elongated.

3.3.2 | Canines

Paranthropus: marked lingual mesial marginal ridge and distal marginal ridge; crown mesiodistally reduced.
Homo: weak lingual mesial marginal ridge and distal marginal ridge; crown mesiodistally elongated.

3.3.3 | Molars

Paranthropus: crown bucco-lingually expanded; bulbous cusps, with curved buccal and lingual faces; marked buccal grooves; accessory cusps present; weak or absent Carabelli trait.
Homo: crown mesiodistal elongated; cusps with vertical buccal and lingual faces; weak buccal grooves; Carabelli trait usually distinct.

3.4 | Mandibular permanent teeth

3.4.1 | Incisors

Paranthropus: crown mesiodistal dimension reduced; I2 with straight incisal edge; faint lingual relief.
Homo: crown mesiodistally elongated; incisal edge curved distally; more marked lingual relief.

3.4.2 | Canines

Paranthropus: weak median ridge; slightly asymmetrical lingual crown profile.
Homo: more marked median ridge; markedly asymmetrical lingual crown profile.

3.4.3 | Premolars

Paranthropus: crown outline bucco-lingually expanded; marked talonid, often with additional cuspulids; buccal face broad at the cervix; long roots.
Homo: crown outline BL reduced; no additional cuspulids; buccal face narrow at the cervix; short roots.

3.4.4 | Molars

Paranthropus: crown outline bucco-lingually expanded; bulbous cusps, with curved buccal and lingual faces; C6 very common; C7 very rare; mesio-buccal groove deep and short.
Homo: crown outline mesiodistal elongated; cusps with vertical buccal and lingual faces; C6 very rare; C7 very common; mesio-buccal groove long.

3.5 | Anatomical descriptions

Abbreviations include: ICF = interproximal contact facet, BL = buccolingual or labiolingual, MD = mesiodistal, M = Mesial, MB = mesiobuccal, DB = distobuccal, L = lingual, ML = mesiolingual, DL = distolingual, IC = incisocervical(lly), DMR = distal marginal ridge, MMR = mesial marginal ridge, and DEJ = dentino-enamel junction. Tooth abbreviations follow these examples: RM_1: Right mandibular permanent first molar; Ldm^1: Left maxillary deciduous first molar. All measurements are in mm.

DNH 27 (b) RP_4 (c) RM_1 (Figure 2). This specimen comprises two isolated, associated teeth: a RM_1 and a RP_4.

RP_4. This tooth is the antimere of DNH 27, now relabeled 27a. Despite differences in color with DNH 27a (a LP_4) this specimen is almost identical in overall morphology, wear, root number, and dimensions of crown and roots. Description of DNH 27a is given in Moggi-Cecchi et al. (2010). Both the crown and roots are well-preserved, except for minor cracks crossing the occlusal surface. This element is worn flat with dentine exposures visible on the protoconid and the metaconid. Tiny dentine pits are also visible on the large talonid, on both the buccal and lingual side. Both the mesial and the distal ICFs are large, reaching the occlusal surface and markedly reducing the original MD dimension. The mesial ICF faces mesio-lingually, whereas the distal ICF faces disto-buccally. This condition suggests that the premolar had a slight abnormal rotation in the tooth row. On the buccal surface remnants of a deep distobuccal groove are evident. Enamel extensions of the cervical margin are evident on the buccal and the lingual face. Both the mesial and distal roots are very long and thin and have two distinct canals. The mesial root is tilted distally. Root length is as follows: M 19.9 mm and D 18.7 mm. The nearly square occlusal outline is typical of the molarized premolars seen in *P. robustus* specimens (e.g., SKW 5, SKX 32162, DNH 7, DNH 8).

RM_1. The tooth is well-preserved, except for a fragment of the crown missing from the mesial face. The occlusal surface is worn to a flat table. A moderate dentine exposure is visible on the entoconid while one large dentine exposure obscures the metaconid, protoconid, hypoconid, and hypoconulid. Enamel extension is evident on the lingual face. The distal ICF is very large, and occupies most of the face. No occlusal morphological details can be described. The mesial roots are very long and thin and the apex is tilted distally. They are partially fused, although two root canals are evident. Similarly, the distal roots are completely fused, straight and the apex tilted distally. Root length is as follows: ML 16.6 MB 16.6 DL 16.9 DB 17.3.

DNH 77b. L_C (Figure 3). This is an isolated and fairly well-preserved tooth. This specimen has been associated with DNH 77a (RI^1) (as published in Moggi-Cecchi et al., 2010) due to similar wear, manganese staining and degree of root resorption. An enamel chip is missing from the labial face. The lingual edge of the occlusal margin is damaged. A crack crosses the occlusal surface and continues over the labial surface of the root to the apex. A flake of cementum is missing on the mesio-labial corner of the root. The crown is heavily worn. This wear has markedly reduced the crown height and exposed a large, subtriangular area of dentine. The large, flat wear plane is lingually and distally tilted. A very thin enamel rim is evident on the labial edge. On the labial face only a few millimeters of enamel are preserved. The enamel line is concave. The root is long and straight and subtriangular in cross-section, mesio-distally compressed. The root tip is tilted lingually with some degree of resorption. Root length is 22.2. Though little to no morphology is preserved, overall dimensions of the preserved parts are suggestive of *P. robustus*.

DNH 79b. L_C (Figure 2). This specimen is an isolated, well-preserved, and unworn tooth. Preservation is good, apart from some abrasion on the labial face. Only a flake of enamel is missing from the lingual face, on the cervical eminence. The crown is intact, with minor cracks. Morphological features of the crown and the marked hypoplastic line on the labial face clearly indicate that this specimen is the antimere of DNH 79a (as published in Moggi-Cecchi et al., 2010). The labial face is tall and convex IC and MD. The crown outline is slightly asymmetrical with the distal edge longer than the mesial edge and

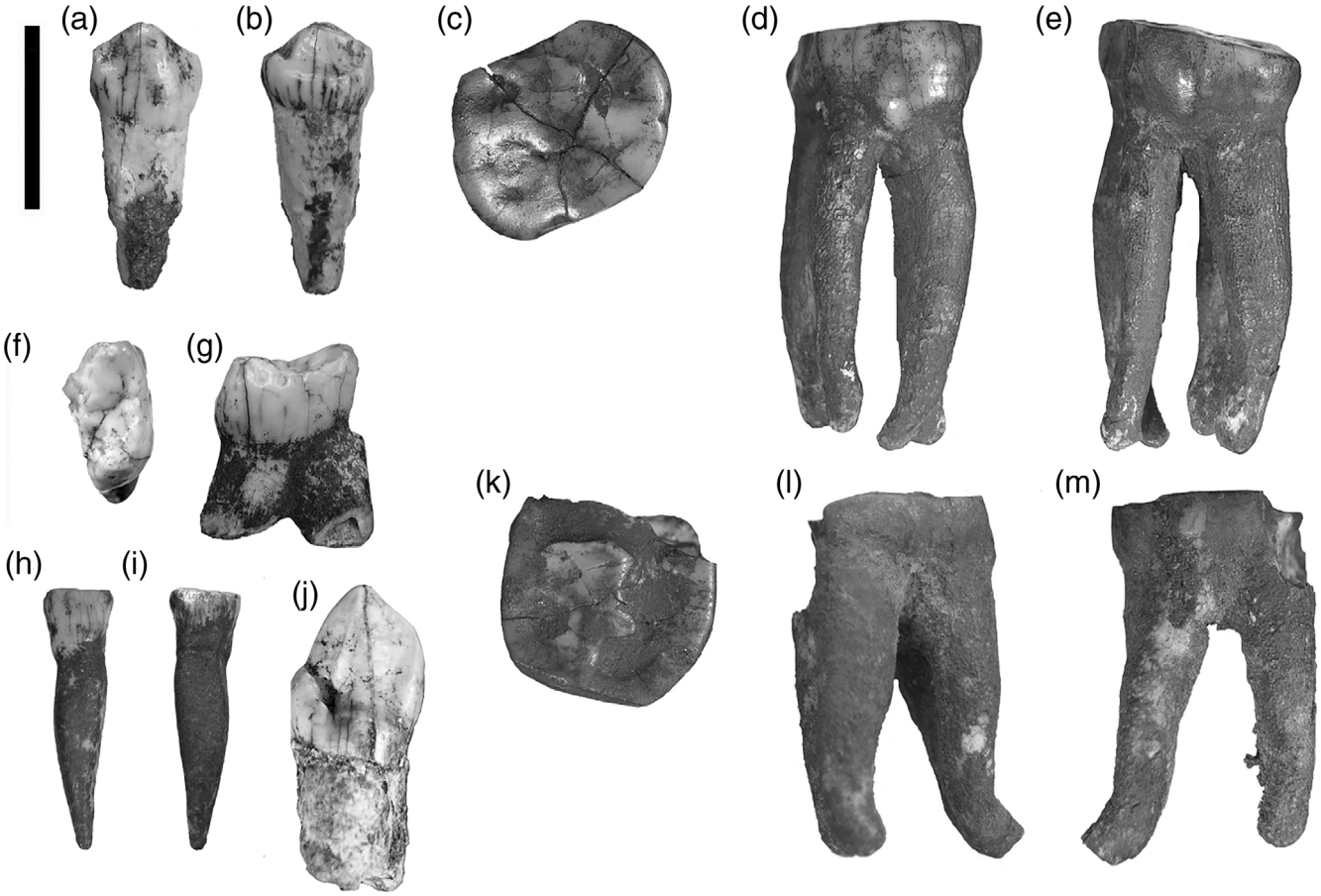

FIGURE 2 (a–b) DNH 87 lingual and labial views; (c–e) DNH 27b occlusal, buccal, and lingual views; (f–g) DNH 85 occlusal and distal views; (h–i) DNH 88 labial and lingual views; (j) DNH 79b lingual view; (k–m) DNH 27c occlusal, buccal, and lingual views

more steeply inclined. The mesial edge is short and angled. The crown tip is centrally placed. The MMR is faint, whereas the DMR is marked, giving rise to an incipient stylid with a deep mesial furrow. The cervical enamel line is straight. A marked line of hypoplasia is evident in the cervical third of the crown. On the lingual face, the cervical eminence is moderately developed. It is distally positioned in respect to the midline and gives rise to a marked DMR with a thin edge. The median lingual ridge is slightly developed, but has a sharp crest which, along with the DMR, delimit a deep, and V-shape cleft. The MMR is relatively faint. The root is thick and oval in section, with MD compression on the mesial face where a subvertical groove is present. 6.8 mm of the still developing root are present. The weak median ridge and the slightly asymmetrical lingual crown profile, coupled with the robusticity of the root, are suggestive of attribution to *P. robustus*.

DNH 85 molar fragment (Figure 2). This is a fragment preserving only the distal part of the crown and part of the roots of a maxillary deciduous molar, probably a Ldm^2. The base of the two roots is not preserved. The distal part of the metacone is present, which is slightly worn. The hypocone is well developed and it has a wear facet on its cusp tip. The posterior fovea is deep. The DMR is low and thick with a centrally located incipient cuspule. On the distal face, an oval ICF is present, although not very marked. Tiny hypoplastic pits are also present. The BD root is MD compressed with a marked groove on its mesial face. Only 6.2 mm of the root are preserved. The preserved part of the lingual root is oval in section. Its length is 5.5 mm. The lack of morphological detail on this fragmentary specimen prevents a reliable taxonomic attribution.

DNH 86 RM_3 (Figure 3). This is an isolated tooth in a small mandibular fragment. Most of the distolingual corner of the crown is missing. Enamel flakes are also missing on the mesiobuccal and the mesiolingual corners. The distal roots are not preserved. The occlusal surface is worn to a flat table. A dentine pit is evident on the metaconid. The mesial ICF is large, concave and occupies most of the face. The occlusal outline is oval, tapering distally. No further morphological details can be described, except for a deep mesiobuccal groove. The mesial roots are long, thick and tilted distally. They are fused, although the two root canals are evident. The ML portion of the preserved root is 17.4 mm. The occlusal outline is similar to that of DNH 8 as well as SKX 5014. The overall size of this specimen, the flat wear, the presence of thick enamel despite advanced wear, and a deep MB groove support the attribution of *P. robustus*.

DNH 87 Ld^C (Figure 2). This is a well-preserved isolated deciduous tooth. Wear has slightly reduced the height of the cusp, and has exposed a pit of dentine. A wear facet is present on the mesial edge

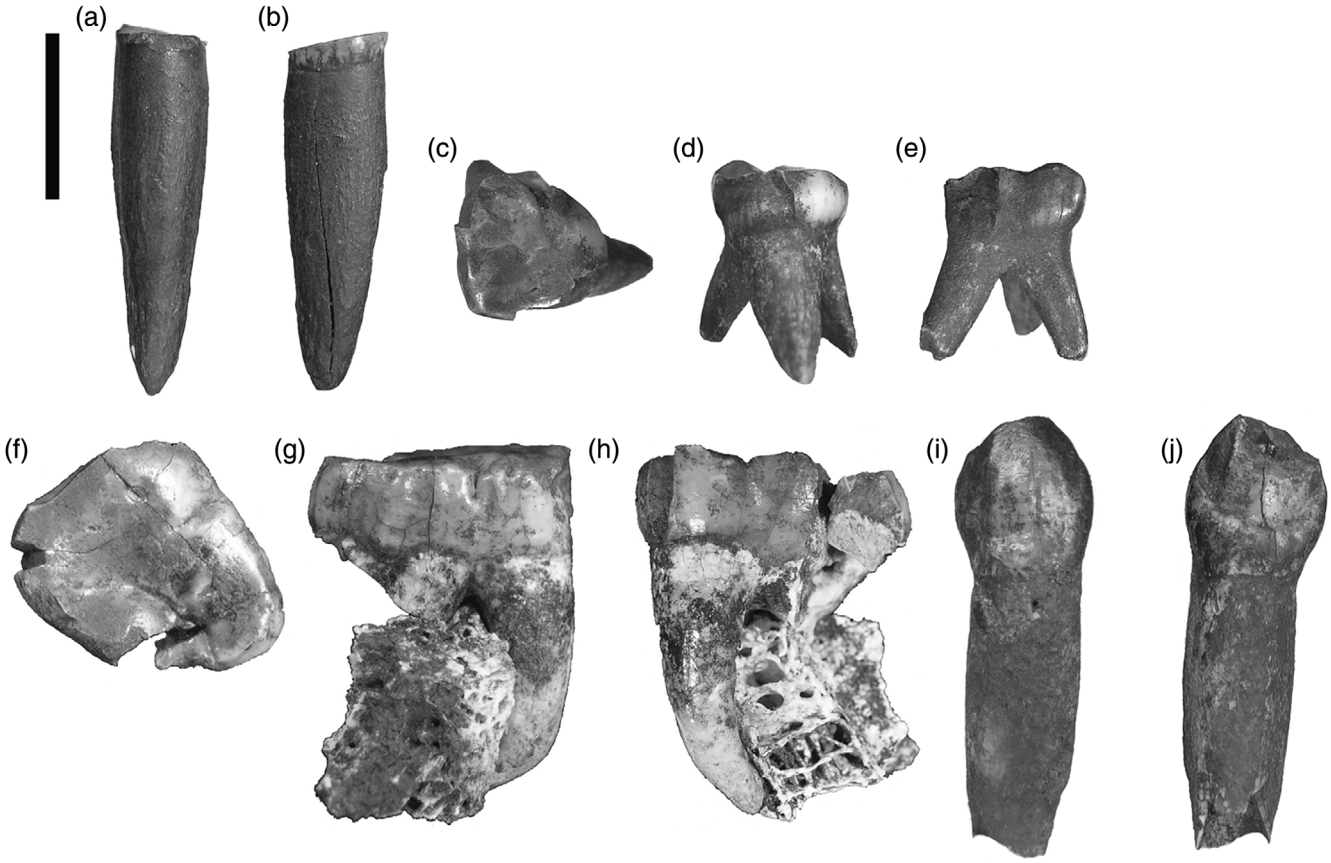

FIGURE 3 (a–b) DNH 77b labial and lingual views; (c–e) DNH 89 occlusal, buccal, and lingual views; (f–h) DNH 86 occlusal, buccal, and lingual views; (i–j) DNH 90 labial and lingual views

of the crown. There is no mesial ICF. The distal ICF is large and subtriangular in shape. The labial crown outline is almost symmetrical. The face is slightly convex in MD direction. The cervical enamel line is slightly asymmetrical, with the apex of the concavity displaced mesially in respect to the cusp tip. The labial MMR and DMR are weakly developed. The MMR is thick and rounded, with a distal cleft. The DMR is thinner than the mesial but evident. A median lingual ridge is evident, and it is placed mesially to the midline. On the lingual face, the cervical eminence is weakly developed and skewed mesially. The root is long and conical in shape, and its apex appears still open. The root is slightly abraded on its lingual side. It shows some degree of resorption on its labial face. Root length is 9.8. Small crown size and buccal face slightly convex MD suggest an attribution to *P. robustus*.

DNH 88 Ldi$_1$ (Figure 2). This is an isolated and well-preserved deciduous tooth. The crown is heavily worn, with a large rectangular area of dentine exposed on the incisal edge. Wear has markedly reduced crown height. The wear plane is tilted slightly labially. The preserved portion of the labial face is straight. On the lingual face the crown outline is triangular and asymmetrical, displaced distally in respect to the midline. A faint cervical eminence is present. A large distal ICF is present while the mesial ICF is not preserved. The root is long and relatively thick, oval in section, with some degree of MD compression. The root tip is tilted slightly mesially and lingually. Root length is 11.7 mm. The reduced crown dimensions point to affinities with *P. robustus*. The specimen is allocated to *P. robustus*?.

DNH 89 Rdm^1 (Figure 3). This is an isolated deciduous tooth. Enamel is missing from half of the mesial face, the mesiobuccal corner, most of the distal face, and half of the lingual face. Wear is marked, with pits of dentine exposed on all cusps. The preserved occlusal outline is almost triangular. The four main cusps are evident, however the relative size of the cusps cannot be accurately assessed. Despite enamel loss, the EDJ morphology suggests the presence of a parastyle, as seen in other examples of this element. The anterior fovea is reduced to a fissure. The central fossa is large. The crista oblique, although worn, is present as a thick and low ridge of enamel. The posterior fovea is a long, transverse fissure that is situated at a different level from the trigon. On the buccal face, the distobuccal groove is faint, ending gradually. There is no tuberculum molare. On the lingual face, there is no evidence of a Carabelli trait. The lingual aspect of the protocone is inflated. The roots are closed and well-preserved. The buccal roots are relatively thick and MD compressed. A deep groove on the mesial face of the MB and the DB roots suggests the presence of a double radicular canal. The lingual root is subconical in shape and subtriangular in section. It is widely divergent from the buccal roots. Preserved root length is: MB: 7.1, DB 7.6; Lingual 9.7. The inflated protocone, lack of tuberculum molare and weak DB groove suggest

attribution to *P. robustus*. Morphological similarities to DNH 36 also support this attribution.

DNH 90 L^C (Figure 3). This is an isolated and overall well-preserved crown and root. The cusp tip is broken, exposing dentine fragments inside. The preserved labial crown outline is symmetrical. The cervical enamel line is slightly asymmetrical, with a concavity located distally in respect to the midline. A hypoplastic band is evident in the upper third of the crown. Lingually, the cervical eminence is strongly developed and skewed mesially, bearing an incipient cuspule. The MMR is thick, with a shallow cleft distal to it. The DMR is also thick, with a deep cleft mesial to it. The median ridge, with a sharp edge, is evident mesial to the midline. A small, oval mesial ICF is evident. There is no distal ICF. The root is long and thick with a MD compression resulting in an oval section view. On its labial face, near the root tip periradicular bands are clearly visible. The root is still open suggesting that the tooth was still developing. Root length is 17.2. The marked lingual MMR and DMR and the dimensions support an attribution to *P. robustus*.

DNH 91 L_C (Figure 4). This is an isolated and overall well-preserved tooth. It is considered here a lower canine, although the crown is greatly reduced, nearly resembling an incisor. The crown was broken in three pieces but has been cleanly refit. A tiny chip of enamel is missing on the apical tip. The labial outline is oval, with some mesioincisal extension. The labial face is tall, markedly convex both IC and MD. On the lingual face, the cervical eminence is weakly developed and placed slightly distal to the midline. The MMR is weakly expressed, whereas the DMR is more marked. A large but not marked mesial ICF is present. The distal ICF is an irregular oval, on the distolingual edge. The root is long and thick, subtriangular in section and MD compressed, with longitudinal grooves on the mesial and distal faces. Numerous periradicular bands are clearly visible. Root apex is still open indicating incomplete development. Root length is 17.6. Overall morphology of this specimen differs from other lower canines of *P. robustus*, in that the labial outline is oval and lacks the typical slightly asymmetrical profile. Taxonomic allocation is *P. robustus*?.

DNH 92 LP_3 (Figure 4). This is an isolated specimen. Preservation is good, excluding an area of abrasion near the cervical margin of the buccal face, affecting the crown and the root. Attrition is minimal with a wear facet on the mesial edge of the buccal cusp. Two adjacent ICF of different size are evident on the buccal face: one smaller, facing mesially, the other larger, facing buccally. This condition suggests that the premolar was misaligned in the tooth row. The overall crown morphology is also irregular, perhaps suggesting a developmental abnormality. The occlusal outline is almost circular, with some buccal extension. The two main cusps are not clearly delineated. There is no anterior fovea. The central fovea is deep and broad forming a round pit. The talonid is large and it bears three incipient cuspulids. Morphological details of the buccal face are obscured by wear. There is a single root, thick and relatively long despite breakage at the tip. It is subtriangular in section and MD compressed, with longitudinal grooves on the mesial and distal faces. These suggest the presence of a double radicular canal. The preserved portion of the root is 16.4. The relatively large talonid and the incipient distal cuspulids are suggestive of allocation to *P. robustus*. However, markedly reduced MD and BL dimensions fall below the minimum for *P robustus* and in the lower range for early *Homo*. Taxonomic allocation is indeterminate.

DNH 93 LI^1 (Figure 4). This is an intact and isolated tooth. On the crown a large flake of enamel is missing from the incisal half of the lingual face. The incisal edge is not preserved. The labial outline is almost trapezoidal. The preserved portion of the labial face is slightly convex both MD and IC. Perikimata are evident throughout the crown. On the lingual face, the cervical eminence is weakly developed with a small groove present distally. A large hypoplastic area is present in the central part of the face. Remnants of the mesial ICF are visible. The distal ICF is elongated, and it is lingually displaced in respect to the midline. The root is long, thick, subtriangular in section, and MD compressed. Root length is 19.5. Damage to the crown precludes description of additional morphological details. The combination of BL expansion and minimal MD breadth supports an attribution to *P. robustus*. Morphological similarities with specimens such as SK 40 also support this attribution.

DNH 94 Ldi^1 (Figure 4). This is an isolated and very well-preserved deciduous tooth. The crown is heavily worn, which has markedly reduced the crown height. A large and concave area of dentine is exposed. The labial face is convex MD and almost straight IC. Hypoplastic pits are present in the central part of the face. On the lingual face, the cervical eminence is marked and centrally placed. A median ridge was likely present before wear, indicated by its sectioned profile at the incisal margin. The mesial ICF is large and circular, occupying most of the mesial face and nearly reaching the incisal margin. The distal ICF is large and concave. The root is thick, conical in shape and BL compressed. Its apex is tilted lingually. There is a longitudinal groove on the labial face. Root length is 10.6. The broad shape of this specimen at the cervix supports an attribution to *P. robustus* as well as it is morphological affinities with specimens such as SWT1/LB-15.

DNH 95 Rdi^2 (Figure 4). This is an isolated deciduous tooth. The crown is intact and unworn. The labial face is subtriangular in outline, with a mesioincisal extension. It is convex both MD and IC. The incisal edge slopes distally. The lingual face shows a weak cervical eminence and poorly developed MMR and DMR. Only a few mm's of the root are preserved on the lingual side. The overall appearance of the tooth suggests that it is developmentally reduced, as sometimes the case in lateral incisors. MD and BL dimensions are very small. This specimen may represent a non-hominin primate.

DNH 96 L and Rdm^1 (Figure 4). This specimen comprises two isolated antimere deciduous teeth. The left tooth is very well-preserved, except for a tiny chip of enamel missing on the mesiolingual corner, near the cervical margin, and a minor crack crossing the lingual cusps. The right tooth has enamel missing from most of the mesial and distal faces as well as on the mesiolingual part on the occlusal surface of the protocone. The roots of both elements are well-preserved. The description of the crown refers to the left tooth.

The crown is worn, with small areas of dentine exposed on the mesial cusps and on the hypocone. The cusp tip of the metacone is rounded, but there is no dentine exposure. The occlusal outline is

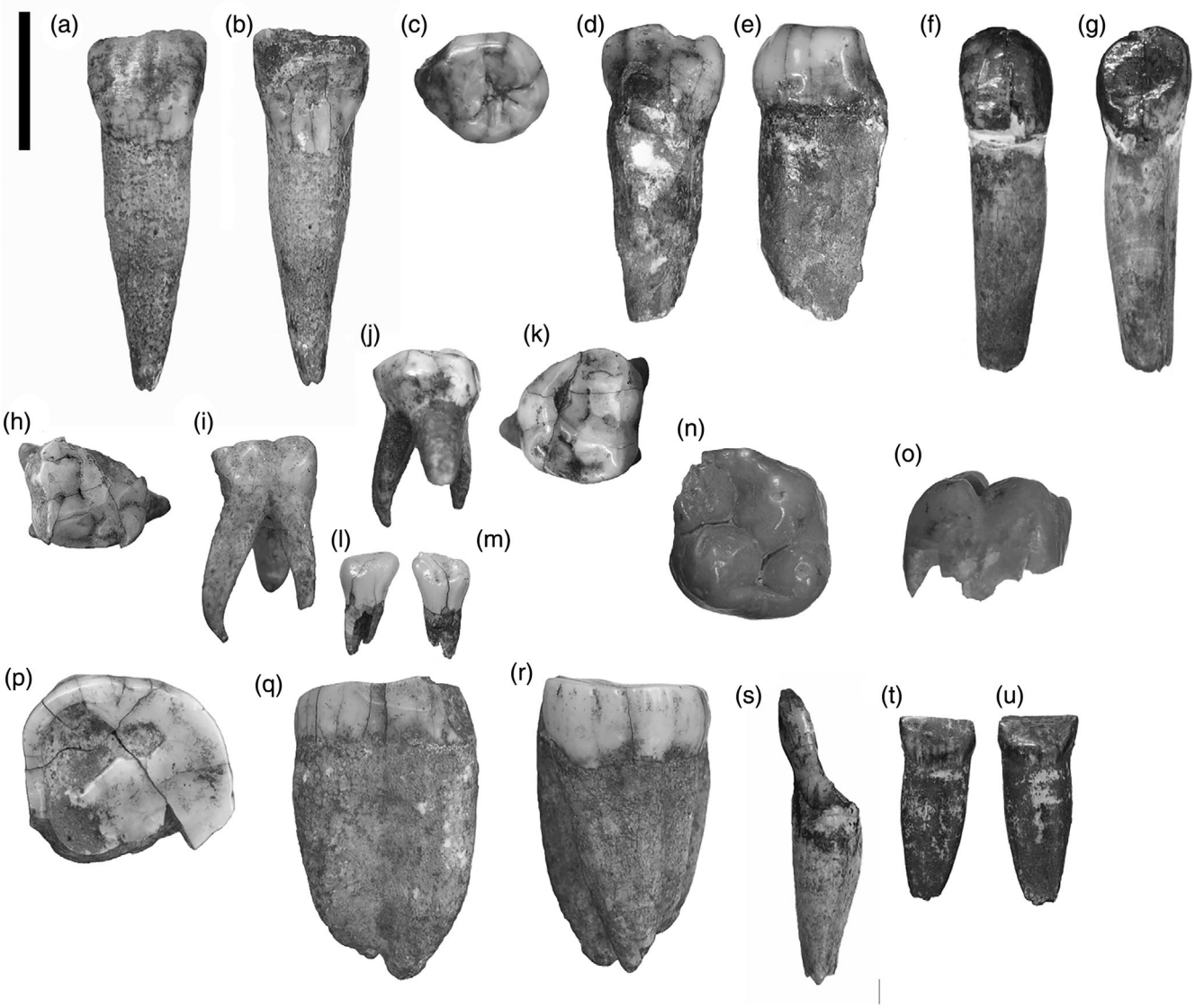

FIGURE 4 (a–b) DNH 93 labial and lingual views; (c–e) DNH 92 occlusal, buccal, and distal views; (f–g) DNH 91 labial and lingual views; (h–i) DNH 96a occlusal and buccal views; (j–k) DNH 96b occlusal and buccal views; (l–m) DNH 95 labial and lingual views; (n–o) DNH 99 occlusal and buccal views; (p–r) DNH 97 occlusal, buccal, and lingual views; (s) DNH 98 labial view; (t–u) DNH 94 labial and lingual views

almost square, with a marked mesiobuccal extension. The four main cusps are evident. The protocone is the largest, followed by the paracone and metacone of approximately similar size and then the hypocone. There is a parastyle that merges with a thick MMR. The anterior fovea is reduced to a fissure and is bounded distally by an enamel ridge emanating from the tip of the paracone. The central fossa is small and deep, partly occupied by an enamel ridge connecting the paracone and the metacone. The crista obliqua is present as a thick ridge of enamel. The posterior fovea is reduced to a shallow fissure by an enamel ridge emanating from the hypocone and is bounded by a worn and thick DMR. No additional cuspules are present. On the buccal face, a faint mesiobuccal groove delineates the parastyle. No tuberculum molare is evident. The distobuccal groove is faint, ending gradually. On the lingual face, the lingual groove is deep and ending gradually. No obvious Carabelli trait is evident. The mesial ICF is circular in shape and buccally placed in respect to the midline. The distal ICF is large, oval, and reaches the occlusal margin. It is slightly lingual in respect to the midline. The MB root is long and it shows two radicular canals with the tip curving lingually. The DB root is short, straight and is oval in cross section. The lingual root is long and conical in shape. It is widely divergent from the buccal roots. The DB and the lingual roots show resorption on their surfaces. Root lengths are as follows: MB 8.9, DB 10.1, L 6.9. A number of features (paracone and metacone of similar size; weak MB groove; lack of tuberculum molare; thick DMR) as well as their morphological affinities with DNH 89 and 36, support an attribution to *P. robustus*.

DNH 97 RM$_3$ (Figure 4). This is an isolated and overall well-preserved tooth. Enamel is missing from most of the lingual face and the mesiolingual corner. The tooth is heavily worn with dentine exposure on the protoconid, metaconid, and the hypoconid created a

single large basin. The remaining cusps are worn flat, with no dentine exposures. The occlusal outline is ovorectangular, with some distolingual extension. The heavy wear precludes description of additional morphological details. On the buccal face, a large hypoplastic area is evident in its central part. There is a large mesial ICF that reaches the occlusal margin. The mesial roots are long, thick, and tilted distally. They are fused with two root canals still evident. Similarly, the distal roots are fused, straight and distally oriented. Root length is: ML 19.6 MB 16.7 DL 17.4 DB 13.6. BL expansion, flat wear, distal tapering and affinities with DNH 18/19 support an attribution to *P. robustus*.

DNH 98 RI^1 (Figure 4). Only a distal fragment of the crown is preserved on this specimen. The root has the tip broken and the labial face abraded. On the crown fragment no morphological details can be described, except for a distal ICF. The incisal edge is also damaged. The preserved portion of the root is long, thick, and subtriangular in section. The preserved root length measured on the labial face is 13.4. The fragmentary nature of this specimen precludes confident taxonomic attribution.

DNH 99 RM^1 (Figure 4). This is an isolated, partial crown of a developing tooth. The mesiobuccal corner of the crown is missing, broken through the paracone. The tooth has enamel chips missing from near the crown base on the lingual and buccal faces. The preserved distal face shows crown completion but no root formation. Occlusal outline appears to have been square, with the four cusps well delineated. The anterior fovea is a short fissure, mesially placed to the paracone and poorly delineated from the large and deep central fovea. The MMR is thin but well developed, bearing two cuspules. The crista oblique is thick but low and is intersected by the longitudinal fissure. The posterior fovea is deep with a trilobate shape and is bounded distally by a low, thin DMR. The lingual groove is shallow, ending abruptly. There is no visible Carabelli trait. No details of the buccal face beyond the presence of the start of the buccal groove can be described. The mesiodistal elongation of the crown and the cusps with vertical buccal and lingual faces suggest affinities with *Homo*. Taxonomic allocation is *Homo*?.

DNH 100 LM$_2$ (Figure 5). This is an isolated and well-preserved tooth. Crown formation is complete with no root formation. An enamel flake is missing on the central part of the lingual face near the cervix. The occlusal outline is ovo-rectangular and slightly compressed MD. The main cusps are well-developed with the metaconid being the largest, followed by the protoconid and hypoconid of similar size. The cusps form a Y pattern. A well-delineated C7 is present, reaching the longitudinal fissure. The MMR is thick and low with three incipient cuspulids present in its central part. One of these cuspulids contacts the fovea anterior, which is large and deep. A continuous distal trigonid crest is evident though it dips very low centrally. The central fossa is broad and deep, intruded upon by enamel extensions from the metaconid, hypoconid, and entoconid. The distal fovea is small but deep, bounded by a thin and low DMR. The mesiobuccal groove is deep and broad, ending into a deep pit. A well-developed protostylid is present. The distobuccal groove is deep and short, terminating in a small pit. Two shallow parallel furrows delimit the C7 and continue down the lingual face in shallow grooves. The mesiodistal elongation of the crown outline, cusps with vertical buccal and lingual faces, lack of C6, presence of C7, and the morphological affinities with DNH 67 support an attribution to *Homo* sp.

DNH 101 RM$_2$ (Figure 5). Crown formation is complete with few millimeters of root formed. Most of the disto-lingual portion of the tooth, including the entoconid and most of the hypoconid, is missing. The occlusal outline appears to have been rectangular with distal tapering on the buccal side. The preserved main cusps are well developed. The metaconid is the largest cusp. The relative size of the others is difficult to assess. The cusps form a Y pattern. On the metaconid a faint groove delineates an incipient postmetaconulid. The MMR is thick and low with a premetaconulid and two mesioconulids evident. The base of the metaconid is separated by the lingual end of the MMR. The anterior fovea is reduced to a thin and deep fissure, bounded by a distal trigonid crest. The latter is incised by the longitudinal fissure. The central fossa is broad and shallow, and is incised by numerous grooves running buccally and lingually from the longitudinal fissure. These additional grooves combined with small enamel expansions from each of the main cusps create a series of small cuspules throughout the central fovea. Both the mesiobuccal and the distobuccal groove are thin and deep with the former ending in a deep pit. The preserved portion of the lingual groove is faint. Root growth is incomplete, extending only a few millimeters from the cervical margin. The deeply incised but narrow mesiobuccal groove and large bulbous cusps support the attribution of this specimen to *P. robustus*.

DNH 102 LI$_2$ and L$_C$ (Figure 5). This specimen comprises two well-preserved, associated, and isolated teeth.

LI$_2$. The developing crown of this element is only half formed. In its most cervical part it shows a "pavement cracking" appearance, typical of immature enamel. The labial face is convex IC and MD. The crown outline is asymmetrical, with an angulated mesio-incisal corner and a more rounded distal corner. In lingual view, the incisal edge has several mamelons of different sizes. The MMR is very faint, whereas the DMR is thick but weakly expressed, ending in a tiny cuspule on the incisal edge. The lingual face is flat both MD and IC. Part of a faint median lingual ridge is also evident.

L$_C$. The crown of this element is also still developing, showing immature enamel. The labial face is markedly convex IC and MD. The crown outline is markedly asymmetrical with the apex distally placed to the midline. The mesial edge is short and angled. The distal edge is much longer than the mesial edge and very steeply inclined. The preserved portion of the MMR is faint, whereas what is present of the DMR is marked, giving rise to an incipient stylid. A broad furrow is evident mesial to the DMR. The median lingual ridge is strongly developed, running distally from the cusp tip as a sharp crest.

The I2 shows mesiodistal elongation of the crown, the distally curved incisal edge, and the presence of mamelons while the C shows a markedly asymmetrical lingual crown profile. These features support the attribution of this specimens to *Homo* sp. Additionally, both elements show morphological affinities with SKX 2354/2355/2356.

DNH 103 I (Figure 5). This specimen is represented by a half crown of a developing lower incisor, possibly I$_1$. Preservation is good.

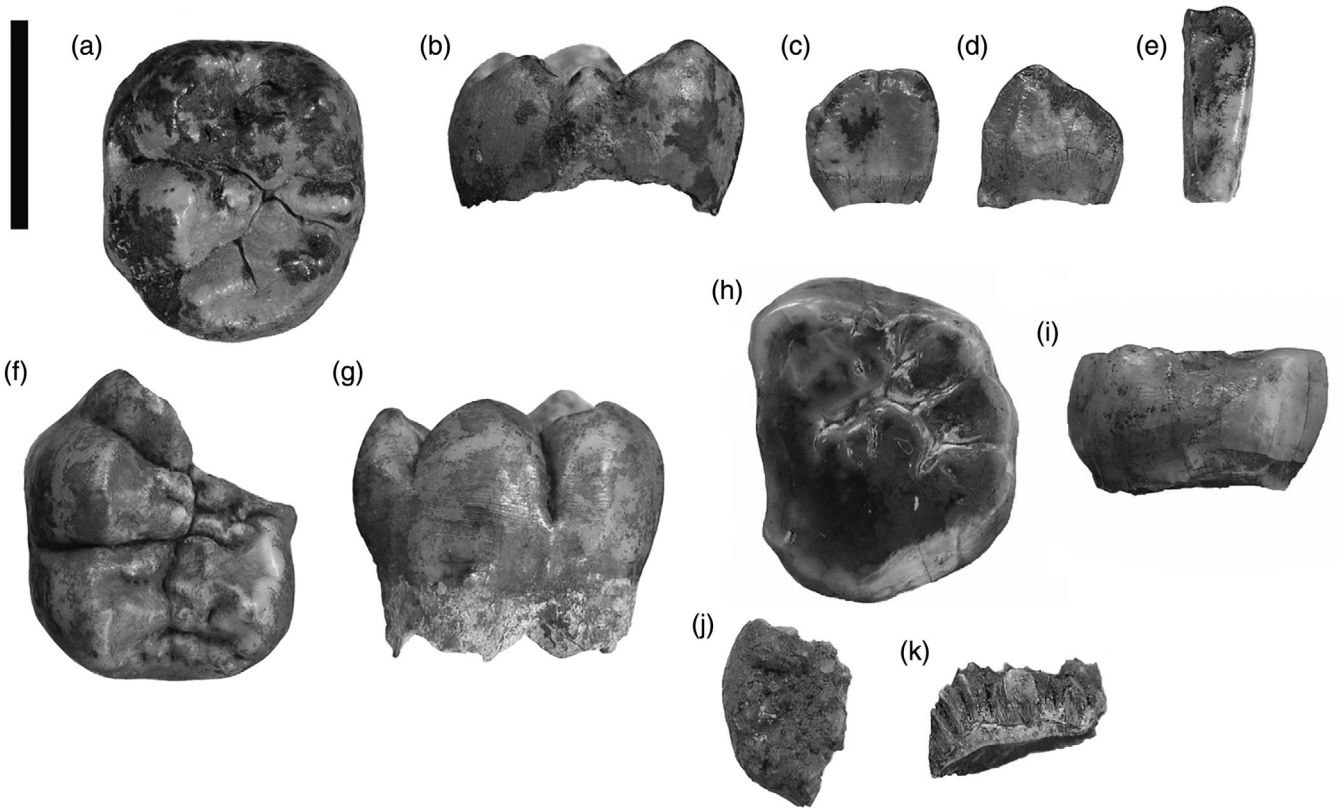

FIGURE 5 (a–b) DNH 100 occlusal and buccal views; (c) DNH 102 I2 lingual view; (d) DNH 102 C lingual view; (e) DNH 103 lingual view; (f–g) DNH 101 occlusal and buccal views; (h–i) DNH 104 occlusal and buccal views; (j–k) DNH 105 occlusal and lateral view

The crown is short of completion. The labial face is tall and almost straight IC. Perikymata are clearly visible. On the lingual face a thick and low marginal ridge is evident. The fragmentary nature of this specimen precludes further morphological assessment.

The fragmentary nature of this specimen precludes confident taxonomic attribution.

DNH 104 LM^3 (Figure 5). This isolated tooth has only the crown preserved and is broken just below the cervix. Preservation is good, except for a large flake of enamel missing from the cervical half of the mesio-lingual face. Wear has reduced the occlusal surface to an almost flat plane, with no dentine exposures. The occlusal outline is almost rounded in appearance. The protocone is the largest cusp, followed by the paracone, hypocone and metacone. Although the crown is worn, a well-developed C5 is still evident, occupying the majority of the posterior fovea. A broad and deep central fossa is present. The crista obliqua is deeply incised by the longitudinal groove. A subvertical furrow on the mesio-lingual corner of the crown suggests the presence of a Carabelli's trait. The mesial ICF is very large and flat, and nearly reaches the occlusal margin. The bucco-lingual expansion of the crown, the occurrence of a C5, a weak Carabelli trait, as well as this specimen's morphological affinities with DNH 18, DNH 19, DNH 15, and SKW 11 support the attribution to *P. robustus*.

DNH 105 Molar fragment (Figure 5). This is a fragment of the crown of a developing molar. The preserved surface shows no morphological details, as the enamel is not yet fully formed. Enamel rods are clearly visible. This specimen cannot be given a taxonomic attribution.

3.6 | Sample composition and taxonomic attributions

Among the 24 new DMQ specimens presented here, some consist of more than one dental element. Thus, the new additions result in 17 new permanent teeth, 7 new deciduous teeth, one incisor that cannot confidently be attributed to maxillary or mandibular, and two molar fragments. The latter is presented here but excluded from any analysis. The new permanent dentition includes one lower I2, four lower C, one lower P3, one lower P4, one lower M1, two lower M2, two lower M3, two upper I1, one upper C, one upper M1, and one upper M3. This new sample also includes one lower di1, one upper di1, one upper di2, one upper dc, and three upper dm1. In particular, the recovery of a lower di1 adds a new tooth class to the sample from DMQ. The new deciduous elements reinforce previous observations that the DMQ assemblage contains a percentage of juvenile specimens that is high as compared to other deposits (Riga et al., 2019). That is, 25.5% of the DMQ dental assemblage consists of deciduous elements. Further, seven of the permanent elements listed above would have belonged to sub-adult individuals (based on developmental stages).

TABLE 1 Taxonomic allocation of new Drimolen dental specimens

Catalogue number	Element	Taxonomic allocation
DNH 27	(b) RP_4 (c) RM_1	*P. robustus*
DNH 77	(b) R_c	*P. robustus*
DNH 79	(b) L_c	*P. robustus*
DNH 85	Molar fragment	Indet.
DNH 86	RM_3	*P. robustus*
DNH 87	Ld^c	*P. robustus*
DNH 88	Ldi_1	*P. robustus*?
DNH 89	Rdm^1	*P. robustus*
DNH 90	L^c	*P. robustus*
DNH 91	L_c	*P. robustus*?
DNH 92	LP_3	Indet.
DNH 93	LI^1	*P. robustus*
DNH 94	Ldi^1	*P. robustus*
DNH 95	Rdi^2	Hominin?
DNH 96	L and Rdm^1	*P. robustus*
DNH 97	RM_3	*P. robustus*
DNH 98	RI^1	Indet.
DNH 99	RM^1	*Homo*?
DNH 100	LM_2	*Homo*
DNH 101	RM_2	*P. robustus*
DNH 102	LI_2 and L_c	*Homo*
DNH 103	Lower I	Indet.
DNH 104	LM^3	*P. robustus*
DNH 105	Molar fragment	Indet.

Specimens in this study were assigned to one of three groups: *P. robustus*, South African early *Homo*, and indeterminate hominin (Table 1). Specimens in the third category consist of fragmentary material, specimens without distinct diagnostic morphology, or specimens whose morphology is unusual such that taxonomic assignment was not determined.

Of these new elements, four permanent teeth have been attributed to the genus *Homo*. This brings the DMQ *Homo* permanent dental sample up to 12, adding to the relatively limited representation of this genus in the Early Pleistocene of South Africa.

4 | COMPARATIVE METRICAL ANALYSIS

4.1 | Materials and methods

A quantitative analysis employing the MD and BL diameters of the *P. robustus* DMQ and the Swartkrans (Member 1, Member 2, Member 3) permanent dental sample is presented here. The largest sample of *P. robustus* specimens has been recovered from Swartkrans, making this a key comparative assemblage for the interpretation of the DMQ material. Metrical data on Swartkrans specimens deriving from different units (Member 1, Member 2, Member 3) have been combined, since it has been shown that no obvious morphological and metrical differences are apparent among specimens deriving from the three deposits (Grine, 1988). The new dental specimens allow for a comparative statistical analysis and the re-examination of the variability between and within the DMQ and Swartkrans assemblages. The analysis presented here is limited to the comparison between the DMQ and the Swartkrans fossil assemblages. Detailed comparisons with samples from other *P. robustus* bearing sites such as Kromdraai B, Coopers D, Gondolin and Sterkfontein have not been carried out due to the small sample sizes from these sites. However, some observations on the Kromdraai B sample are presented in the Discussion section.

Data for the majority of teeth from DMQ (Keyser et al., 2000; Moggi-Cecchi et al., 2010; this paper) were collected by JM-C. Data on DNH 152 and DNH 155 were collected by ABL (Herries et al., 2020; Martin et al., 2021). Data for teeth from Swartkrans recovered prior to 2009 were collected by JM-C. Metrical data on teeth from Swartkrans published after 2009 were taken from the literature (Pickering et al., 2012, 2016; Sutton et al., 2009). The analysis we present here focuses on summary statistics (e.g., mean, range, CV, etc.) that capture information about the properties of the samples. Adjusted coefficient of variation (V^*) was calculated following Sokal and Braumann (1980) for specimens with $n > 1$ and $n \leq 5$. A series of univariate, non-parametric statistical comparisons (i.e., Mann–Whitney U tests) were performed using R (R Core Team, 2017) to test for differences in MD and BL dimensions of the permanent teeth belonging to each assemblage. We further tested the relative variation between samples using a modified version of the Levene's test (Schultz, 1985) indicated as "mratio" in Donnelly and Kramer (1999).

Due to the small sample size, the DMQ early *Homo* and deciduous *P. robustus* dentition were excluded from the latter analyses.

Comparisons between the two major sample of *P. robustus* (DMQ e Swartkrans) are limited here to the basic metrical differences. A more comprehensive and detailed analysis of the potential morphological differences is beyond the scope of this paper. In this regard, data collection aimed at a morphological comparison among the *P. robustus* samples from the main fossil sites in terms of discrete dental traits is presently under way.

5 | RESULTS AND DISCUSSION

Measurements of the new DMQ dental specimens are presented in Table 2. Descriptive statistics for both the expanded *P. robustus* DMQ (Table 3 and Table 4) and the South African early *Homo* samples (Table 5) are also presented. Updated statistics for the expanded *P. robustus* Swartkrans sample are presented in the Supporting Information (Tables S1 and S2). Mean values, coefficients of variation and p values of the statistical comparisons between the permanent dental sample from Drimolen Main Quarry (DMQ) and Swartkrans (SK) are presented in Table 6. The addition of the new *Paranthropus* specimens

TABLE 2 Measurements (in mm) of new Drimolen dental specimens

DNH	Taxonomic allocation	Tooth	MD meas.	MD est.	BL meas.
Maxillary permanent teeth					
DNH 93	*P. robustus*	LI^1		8.8	7.1
DNH 98	Indet	RI^1			
DNH 90	*P. robustus*	L^C		8.6	8.1
DNH 99	*Homo*?	RM^1		12.1	12.2
DNH 104	*P. robustus*	LM^3	13.1	14	15.5
Mandibular permanent teeth					
DNH 102	*Homo*	LI_2		6.8	
DNH 102	*Homo*	L_C	7.01	8.1	
DNH 77b	*P. robustus*	R_C	(6.4)	ND	(8.8)
DNH 79b	*P. robustus*	L_C		7.4	8.4
DNH 91	*P. robustus*?	L_C		7.2	7.5
DNH 92	Indet	LP_3		8.7	9.9
DNH 27 (b)	*P. robustus*	RP_4	9.7		12.5
DNH 27 (c)	*P. robustus*	RM_1			11.8
DNH 100	*Homo*	LM_2		14.9	12.9
DNH 101	*P. robustus*	RM_2	15.3		13.6
DNH 86	*P. robustus*	RM_3	16.5	17.2	14.2
DNH 97	*P. robustus*	RM_3	14.9	15.8	
Maxillary deciduous teeth					
DNH 87	*P. robustus*	Ld^c		6.3	5.2
DNH 89	*P. robustus*	Rdm^1	8.8		9.3
DNH 94	*P. robustus*	Ldi^1	6.1	6.3	4.2
DNH 95	Hominin?	Rdi^2		4.1	3.3
DNH 96	*P. robustus*	Rdm^1	8.3		9.4
DNH 96	*P. robustus*	Ldm^1	8.6	8.7	8.9
Mandibular deciduous teeth					
DNH 88	*P. robustus*?	Ldi_1	3.8		3.5

Note: Measurements of specimens whose taxonomic allocation is tentative (with a "?") or Indet. have been omitted from the summary statistics and metrical analysis. Measurements in brackets are indicative and have been omitted as well.

to the DMQ hominin assemblage allows for a reassessment of the metrical patterns of the Drimolen *P. robustus* dental assemblage as well as for a comparison to the hominin assemblage from Swartkrans, which has also increased in number since Moggi-Cecchi et al. (2010) first undertook this analysis.

5.1 | Central tendency

Among the variables (MD and BL diameters for permanent maxillary and mandibular teeth), the mean values of the Swartkrans assemblage are higher than those for the DMQ site-sample in 26 of the 32 cases (81%; notably including all maxillary teeth) and identical for three variables. Among the deciduous teeth, of the 14 possible comparisons, the mean values for the Swartkrans site-sample are higher than the DMQ sample for 9 variables (64%) and identical for one variable.

A series of univariate, non-parametric statistical comparisons (i.e., Mann–Whitney U tests) were performed to test for statistically significant differences in MD and BL dimensions of the permanent teeth between the two samples (Table 6). Among the maxillary anterior teeth, only the MD of I^2 is statistically significantly different. When comparing the posterior teeth, a more interesting pattern emerges in that all the comparisons are statistically significant different except for the MD of M^2 and the BL of M^1. In the mandibular dentition, no statistically significant differences appear except for the BL of M_2.

In the comparison between the mean values of the DMQ sample and the mean values of the small Kromdraai B sample (often represented by a single tooth) no consistent pattern emerges. Rather, the maxillary teeth the DMQ diameters tend to be larger than the Kromdraai diameters, whereas the opposite is true in the mandibular dentition.

TABLE 3 Descriptive statistics of the Drimolen *P. robustus* permanent dental sample. Measurements in mm

		MD						BL				
Maxillary	*n*	Mean	Min	Max	SD	*V**	*n*	Mean	Min	Max	SD	*V**
I1	4	8.5	8	8.9	0.4	5.1	3	6.8	6.5	7.1	0.3	4.9
I2	3	5.7	5	6.3	0.7	12.5	3	6.1	5.4	7	0.8	14.5
C	6	8.7	7.9	9.9	0.7	8.6	8	8.8	7.9	9.9	0.8	9.1
P3	4	9.2	9	9.7	0.3	3.9	3	13	12.8	13.4	0.3	2.7
P4	4	9.8	9.2	10.1	0.4	4.6	4	13.9	13.6	14.3	0.3	2.2
M1	5	12.8	12	14.1	0.8	6.4	5	14.2	13.6	15.2	0.7	4.9
M2	5	13.1	11.6	15	1.3	10.2	5	14.7	14	16	0.8	5.7
M3	7	13.7	12.1	14.8	0.9	6.8	7	15.3	14.2	16.4	0.8	5.4
		MD						BL				
Mandibular	*n*	Mean	Min	Max	SD	*V**	*n*	Mean	Min	Max	SD	*V**
I1	1	4.3	4.3	4.3	–	–	1	6.1	6.1	6.1	–	–
I2	2	5.5	5.4	5.6	0.1	2.9	2	6.2	5.9	6.5	0.4	7.7
C	4	7.6	7.3	8.1	0.4	5.2	4	8.3	7.6	8.8	0.5	6.5
P3	5	10.3	9.2	11	0.7	7.5	4	12.3	11.3	12.9	0.7	6
P4	8	11	9.8	12.3	0.7	6.7	6	12.9	12.5	13.6	0.4	3.3
M1	6	14.4	13.4	15.7	0.8	5.8	6	12.9	11.8	14.5	1	7.9
M2	8	15.6	13.4	17.2	1.3	8.1	7	14	13	15.2	0.8	5.7
M3	9	16.5	14.3	19.1	1.4	8.6	8	14.4	13.4	16.2	1	7.1

TABLE 4 Descriptive statistics of the Drimolen *P. robustus* deciduous dental sample. Measurements in mm

		MD						BL				
Maxillary	*n*	Mean	Min	Max	SD	*V**	*n*	Mean	Min	Max	SD	*V**
di1	2	6.3	6.3	6.3	–	–	2	4.3	4.2	4.3	0.1	1.7
di2	2	4.6	4.3	4.9	0.4	9.2	2	3.9	3.7	4	0.2	5.5
dc	3	6.1	5.7	6.3	0.3	5.3	2	5.6	5.2	6	0.6	10.1
dm1	3	9.5	8.7	10.1	0.7	7.7	5	9.4	8.9	9.9	0.5	4.9
dm2	3	11.5	11.1	11.8	0.4	3.1	4	11.8	11.1	12.7	0.7	6.2
		MD						BL				
Mandibular	*n*	Mean	Min	Max	SD	*V**	*n*	Mean	Min	Max	SD	*V**
di1	–	–	–	–	–	–	–	–	–	–	–	–
di2	–	–	–	–	–	–	–	–	–	–	–	–
dc	1	3.9	3.9	3.9	–	–	2	4.9	4.9	4.9	–	–
dm1	3	10.34	9.4	11	0.9	8.2	3	8.4	7.7	8.8	0.6	7.0
dm2	3	11.8	11.5	12.2	0.4	3.2	4	10.1	9.9	10.3	0.2	1.6

5.2 | Range

When looking at the distribution of the individual values, the DMQ sample is consistently smaller than the Swartkrans sample. Another way to examine distribution differences between the DMQ and Swartkrans permanent dental sample, is through boxplots of these variables (Figures S1–S6). In the maxillary teeth, with a few exceptions—mostly anterior teeth—the DMQ range largely overlaps the lower end of the Swartkrans range. This condition mirrors the results of the mean values analysis. In the mandibular dentition the DMQ range overlaps the lower end of the Swartkrans range for a few variables (e.g., I_2, M_1, M_2), whereas others show much more overlap (e.g., C, P_3, P_4, M_3). No consistent pattern emerges from the inspection of the boxplots of the deciduous dentition (Figures S7–S10). This is almost certainly due to the limitations of small sample sizes.

TABLE 5 Descriptive statistics of the South African early *Homo* permanent dental sample. Measurements in mm

		MD						BL				
Maxillary	***n***	**Mean**	**Min**	**Max**	**SD**	***V****	***n***	**Mean**	**Min**	**Max**	**SD**	***V****
I1	5	10.4	9.4	11.9	1.0	9.9	3	7.2	6.5	7.6	0.6	8.1
I2	6	6.9	5.5	7.8	0.9	13.2	5	6.9	6.1	7.5	0.6	8.7
C	3	10.0	9.3	10.7	0.7	7.1	2	9.5	8.8	10.3	1.1	11.0
P3	3	9.0	8.6	9.6	0.5	5.4	2	12.3	11.2	13.3	1.5	12.2
P4	1	9.4	9.4	9.4	–	–	0	–	–	–	–	–
M1	9	13.2	12.7	13.9	0.5	3.6	8	13.0	12.2	13.4	0.4	3.2
M2	4	13.2	12.5	13.7	0.5	3.9	4	14.8	14.3	15.1	0.4	2.6
M3	1	13.3	13.3	13.3	–	–	1	16.8	16.8	16.8	–	–
		MD						**BL**				
Mandibular	***n***	**Mean**	**Min**	**Max**	**SD**	***V****	***n***	**Mean**	**Min**	**Max**	**SD**	***V****
I1	2	6.0	6.0	6.0	0.0	0.5	1	5.8	5.8	5.8	–	–
I2	6	7.0	6.4	7.8	0.5	6.6	1	7.0	7.0	7.0	–	–
C	4	8.3	8.1	8.5	0.2	2.0	2	8.6	8.2	9.0	0.6	6.4
P3	3	9.4	8.8	10.1	0.7	6.9	3	10.3	9.9	11.1	0.7	6.6
P4	2	9.6	9.5	9.6	0.1	0.7	2	10.2	10.0	10.3	0.2	2.1
M1	5	13.9	13.3	14.6	0.5	3.8	5	12.0	11.8	12.4	0.3	2.1
M2	3	14.4	14.2	14.9	0.4	2.8	3	12.7	12.2	13.0	0.4	3.4
M3	2	14.9	14.5	15.2	0.5	3.3	1	12.2	12.2	12.2	–	–

TABLE 6 Mean values and coefficients of variation (CV or *V**) of the *P. robustus* permanent dental sample from Drimolen Main Quarry (DMQ) and Swartkrans (SK).

	Mean			Mean			*i**			*V**		
	MD DMQ	**MD SK**	***p* value**	**BL DMQ**	**BL SK**	***p* value**	**MD DMQ**	**MD SK**	***p* value**	**BL DMQ**	**BL SK**	***p* value**
Maxillary												
I1	8.5	8.9	0.08	6.8	7.3	0.42	5.1	8.4	***0.01***	4.9	6.8	***0.01***
I2	5.7	6.5	***0.03***	6.1	6.6	0.76	12.5	10.1	0.39	14.5	9.1	0.94
C	8.7	8.5	0.79	8.8	9.3	0.14	8.6	6.6	***0.00***	9.1	7.9	***0.04***
P3	9.2	9.9	***0.02***	13	14.2	***0.01***	3.9	5	***0.00***	2.7	4.9	***0.00***
P4	9.8	10.6	***0.02***	13.9	15	***0.01***	4.6	5.5	***0.02***	2.2	5.6	***0.02***
M1	12.8	13.3	***0.04***	14.2	14.9	0.06	6.4	5	***0.02***	4.9	4	***0.01***
M2	13.1	14.1	0.08	14.7	15.9	***0.02***	10.2	6.1	0.11	5.7	5.3	0.05
M3	13.7	14.9	***0.03***	15.3	17	***0.00***	6.8	7.6	***0.02***	5.4	3.8	0.07
Mandibular												
I1	4.3	5.5	0.16	6.1	6.3	0.69	–	4		–	6.8	
I2	5.5	6	0.09	6.2	7	0.12	2.9	7	0.11	7.7	5.7	0.74
C	7.6	7.6	0.95	8.3	7.9	0.19	5.2	7.6	0.95	6.5	8.3	0.80
P3	10.3	10.1	0.66	12.3	11.8	0.36	7.5	5.5	***0.00***	6	6.7	***0.02***
P4	11	11.3	0.76	12.9	12.9	0.76	6.7	5.5	***0.00***	3.3	8.1	0.18
M1	14.4	15	0.08	12.9	13.7	0.08	5.8	5.1	0.77	7.9	6.1	0.13
M2	15.6	16.5	0.10	14	15	***0.03***	8.1	5.1	0.22	5.7	6.5	0.45
M3	16.5	17.1	0.20	14.4	14.4	0.67	8.6	4.8	0.33	7.1	5.7	0.59

Note: *p* value of the statistical comparisons between the DMQ and the SK samples are indicated. *p* values < 0.05 are in bold and italics.

5.3 | Variation

Another potential difference between the DMQ and the Swartkrans samples is how size values are distributed across the range, as expressed by the coefficient of variation (CV) or, in the case of samples where $n > 1$ and $n \leq 5$, the V* (following Sokal & Braumann, 1980).

The mean CV across the permanent dentition (MD and BL) of the DMQ *P. robustus* sample is 6.6 (maxillary teeth 6.8, mandibular teeth 6.5) while it is 6.3 for Swartkrans (maxillary teeth 6.4, mandibular teeth 6.2). Though the overall CV value of DMQ is higher than that of Swartkrans, the CV of the Swartkrans *P. robustus* maxillary sample is significantly higher than the DMQ maxillary sample in 7 out of the 16 comparisons (44%); DMQ is higher in 9/16 or 56% of which 4 (i.e., MD and BL of C^1 and M^1) are significant (Table 6). The CV of the Swartkrans *P. robustus* mandibular sample is higher than the DMQ mandibular sample with similar frequency (6 out of the 14 possible comparisons or 43%). of which only the BL of P_3 is significant: DMQ has higher CV values in just over half of the cases. The CVs for the MD of P_3 and P_4 for the DMQ sample are significantly higher than those from Swartkrans, but eleven other comparisons are non-significant.

The picture that emerges from analyzing this expanded sample is that CV values for the DMQ dental sample are higher than the Swartkrans samples. That said, the CV of the DMQ sample has decreased with additional specimens (from 6.9 to 6.6) whereas it increased for the Swartkrans sample (from 6.1 to 6.3; Moggi-Cecchi et al., 2010). Overall, DMQ has higher CV values in slightly more than half of the comparisons. When comparing CV values by tooth classes (I, C, P, M), a similar pattern emerges. CV values in DMQ are smaller than our previous analysis, though still higher than the Swartkrans sample, except for the premolar class.

Differences in dental metrics and variation patterns between the two samples were first noted by Moggi-Cecchi et al. (2010) who suggested that these differences may possibly relate to sampling bias in the Swartkrans sample. This sampling bias was hypothesized to be due to selective accumulation of larger-sized individuals at Swartkrans as a result of predation from large carnivores (e.g., Brain, 1981, 1993). In an effort to test this hypothesis, a preliminary analysis comparing the distributions of the ages at death in the Swartkrans and DMQ samples was recently carried out (Riga et al., 2019). Differences in frequencies of the age-at-death categories were found to suggest different mechanisms of hominin skeletal accumulation at DMQ and Swartkrans. The Swartkrans demographic curve is consistent with mortality in a population subjected to predation, and thus is consistent with the carnivore-accumulating hypothesis. In contrast, the DMQ demographic curve is similar to that of wild populations of living apes, consistent with natural mortality in a population of hominins living around the cave site (Riga et al., 2019). These paleodemographic profiles support the hypothesis of differential collection processes that may lead to biased comparative samples.

More recently, the analysis of the newly discovered DNH 155 *P. robustus* male cranium (Martin et al., 2021), together with a more secure dating of the DMQ deposits (in a broader framework of dating of South African sites; Herries et al., 2020), has led to the hypothesis that differences in cranial morphology and dental metrics between the DMQ and the Swartkrans Member 1 Hanging Remnant (Mb1 HR) specimens might instead be attributed to microevolutionary processes occurring in the *P. robustus* lineage in South Africa. This hypothesis predicts that the DMQ and Swartkrans Mb1 HR assemblages represent time-successive populations of *P. robustus*, in which an increase in dental size has occurred from the older DMQ population to the younger Swartkrans Mb1 HR population. Martin et al. (2021) also identified a suite of qualitative cranial character traits that distinguish the Drimolen sample from the Swartkrans sample, in line with the description of the DNH 7 skull by Rak et al. (2021) who consider this specimen at the primitive pole of the *Paranthropus* morphocline.

The differential sampling hypothesis presented by Moggi-Cecchi et al. (2010) and above hinges on the comparative analysis of the dental dimensions between the DMQ and the Swartkrans assemblage. The microevolutionary hypothesis presented by Martin et al. (2021) employs these metrics as well as metrical and morphological comparison of cranial remains. However, the two types of analyses are not strictly comparable in their dental analyses, because of the differences in comparative samples: Martin et al. (2021) compared the DMQ *P. robustus* assemblage (2.04–1.95 Ma) to the Swartkrans Mb1 HR assemblage only while Moggi-Cecchi et al. (2010) and the one presented above compared the DMQ assemblage to the entire Swartkrans *P. robustus* assemblage (Member 1HR + LB, Member 2 and Member 3). This implies differential temporal controls between the two studies where the former used a dataset for Swartkrans constrained to an older sample, whereas the latter utilized a Swartkrans sample that may include temporal overlap.

The current understanding of the chronology of the *P. robustus* bearing Swartkrans deposits (Member 1 to Member 3) is that they formed over a very long period of time between ~2.2 and around about 1.0 Ma. Swartkrans Member 1 Lower Bank (Mb 1 LB) has been dated by cosmogenic nuclide burial dating to 2.22 ± 0.09 Ma and 1.80 ± 0.09 Ma (Gibbon et al., 2014; Kuman et al., 2021). These ages are very similar to uranium-lead dates of 2.25 ± 0.08 Ma and 1.80 ± 0.01 Ma that underlie and cap the entirety of the Member 1 deposits (Pickering et al., 2019) suggesting that Mb 1 LB formed over a long period of time. Yet only a handful of *P. robustus* specimens, mostly isolated teeth, and a single specimen of *Homo*, have been recovered from this unit (Grine, 1989; Pickering et al., 2016). The oldest *Paranthropus* specimens from Mb1 LB are ~2.2 Ma, whereas the *Homo* specimen is younger. These ages for Mb1 LB imply that the overlying Swartkrans Member 1 Hanging Remnant (Mb1 HR) should date to between 1.89 and 1.79 Ma (age uncertainty of youngest cosmogenic age from Mb1 LB and the U–Pb age of the speleothem that caps Mb1 HR), making it younger than DMQ. As Herries and Adams (2013) note the ~2.25 Ma speleothem directly underlying the Mb1 HR is also heavily truncated suggesting a significant time gap. In contrast the M1b LB, Mb 1 HR has yielded the largest number of *P. robustus* specimens from South Africa including a

number of more complete crania (e.g. SK 46, SK48; Broom & Robinson, 1952), as well as specimens of *Homo* such as SK 847 (Clarke et al., 1970). ESR ages from Mb 1 HR also suggest the deposits are younger than 2 Ma (Curnoe et al., 2001). In contrast ages for Member 2 are 1.36 ± 0.29 Ma based off an experimental dating of fossil material using U–Pb (Balter et al., 2008) and between 224 and 98 ka based on ESR (Curnoe et al., 2001). The discrepancy in these ages is likely due to the fact that much younger units have previously been mistakenly defined as being part of Member 2, such as the ~11 ka old Bondi Channel now defined as Member 5 (Brain, 1993). The nature and age of Member 2 is thus not well defined but it is certainly younger than ~1.8 Ma based on the fact it infilled void space eroded through Member 1 (Brain, 1993). In contrast Member 3 has been dated by U–Pb of fossils, ESR and cosmogenic nuclide burial dating and all three suggest and age between 1.0 and 0.8 Ma (Balter et al., 2008; Blackwell, 1994; Gibbon et al., 2014). This handful of *P. robustus* fossils are the youngest known from South Africa.

This chronology implies differential temporal controls between the two studies where the Martin et al. (2021) study used a dataset for Swartkrans constrained to an age around 1.9–1.8 Ma and thus younger than DMQ, whereas Moggi-Cecchi et al. (2010) utilized a Swartkrans sample that likely includes fossils that are older, potentially the same age as and a lot younger than DMQ, spanning as much as 1.3 Ma. Further, we must also be aware that some patterns identified in the metrical analysis may be the result of small sample sizes rather than true biological patterns. That is as larger specimens are added to the DMQ assemblage and smaller specimens are added to the Swartkrans assemblage (see Pickering et al., 2016), the differences between these two assemblages may become less distinct.

In this framework, the *Paranthropus robustus* dental sample from Kromdraai B could provide key information as a third site bearing *Paranthropus* fossils in the Cradle of Humankind. This is especially true in light of the proposal by Grine (1985, 1988) that the Kromdraai B *Paranthropus* sample should be considered ancestral to the Swartkrans sample—considered by him and by Howell (1978) as two separate, time successive species. Following Broom and Robinson (1952) the Swartkrans sample would be defined as *P. crassidens*. If this were true, it would weigh on both hypotheses discussed above. Unfortunately, analysis of the limited dental metrical evidence from Kromdraai B, although critical, does not provide any precise answers to this question. An expanded sample deriving from Kromdraai B is needed before this can be confidently addressed. Lastly, temporal placement of the different fossil bearing deposits within the Kromdraai complex is still not well defined. Partridge (1982) considered all the fossil hominin material to have been recovered from Member 3 in his stratigraphic analysis. Herries et al. (2009) suggested that Member 3 (which Partridge considered to be younger than Member 1 and 2) would date to <1.78 Ma making the fossils younger than Swartkrans Member 1. This was based on paleomagnetic work by Thackeray et al. (2002) who suggested samples from Member 1 and 2 (although they did not show which deposits the various samples came from) covered the period across the Olduvai subchron (1.95–1.78 Ma). However, since this work, Braga et al. (2013, 2017), Braga, Fourvel, et al. (2016), and Braga, Dumoncel, et al. (2016) have significantly revised the stratigraphy of the site defining 7 Members and have stated that some of the previously discovered hominin material (including TM 1517) come from Members 4 to 6. Braga et al. (2013), Braga, Fourvel, et al. (2016), and Braga, Dumoncel, et al. (2016) suggest that a hominin specimen, KB 5522, may relate to the TM 1517 type specimen and comes from Member 5 above a reversed polarity flowstone that Thackeray et al. (2002) attributed to the period prior to 1.95 Ma. Deposits overlying this flowstone record normal polarity and would thus be dated to the Olduvai Subchron between 1.95 and 1.78 Ma. This would make TM 1517 and other fossils potentially from Member 5 and 6 younger than DMQ, but perhaps older than Swartkrans Mb 1 HR. An ESR date from the deposits younger than the flowstone gave a very young age of 0.81 ± 0.03 Ma (Curnoe et al., 2002) that could suggest, like Swartkrans, that the Kromdraai deposits span a very broad period of time. New excavations at Kromdraai B have yielded hominin material from Member 2 (Braga, Dumoncel, et al., 2016; Braga, Fourvel, et al., 2016), which is now being referred to as Unit P as the Kromdraai team move away from the numbered member system (Ngoloyi et al., 2020). Unit P/Member 2 is suggested to date closer to 2 Ma by Braga, Fourvel, et al. (2016) and Braga, Dumoncel, et al. (2016). Firmer dates and new fossil announcements (e.g., Braga, Dumoncel, et al., 2016; Braga, Fourvel, et al., 2016) might shed new light on this site and provide a clearer picture of *Paranthropus* evolution in South Africa. Several of the hominin fossils remain unprovenanced because they come from decalcified deposits or are ex situ and it is therefore difficult to correlate them to a specific Member (Braga, Dumoncel, et al., 2016; Bruxelles et al., 2016).

From the above discussion it is apparent that taken together, the fossil evidence from the three most important *P. robustus* samples - that is those from the sites of Swartkrans, Drimolen and Kromdraai - provides information on several aspects of the biology and evolution of *P. robustus*. No consistent pattern seems to emerge yet that allows elucidation of the similarities or differences among the three dental samples as a whole. This maybe in part due to the fact that the DMQ *Paranthropus* represent variation over a short window of time (2.04–1.95 Ma), whereas those from Swartkrans as a whole and Kromdraai B represent large temporal variation over as much as a million years. The exception is Swartkrans Mb 1 HR that may date to a similarly short period of time (~1.9–1.8 Ma) to DMQ. Given Swartkrans Mb1 HR and DMQ represent the largest collections of *Paranthropus* comparisons between the two are critical for confirming potential temporal changes within the species as suggested by Martin et al. (2021).

Several factors still limit the possibility to obtain a clear, uniform and consistent picture of the biology, taxonomy and evolution of *P. robustus*. These factors include: 1). A precise chronological framework of the different deposits at the sites. Whereas a firm chronology of the DMQ deposit has been recently established (Herries et al., 2020), dating of the different members at Swartkrans and Kromdraai B is still a matter of debate. 2). The number of fossil specimens recovered from the three sites is very different, as illustrated, for example, by the dental specimens, for which only the entire Swartkrans sample has a numerosity with $n > 10$ for the majority of

tooth classes. This situation, as we have seen above in the comparison between the DMQ and Swartkrans samples, requires caution in the interpretation of the results. The same applies, more so, in any comparison with the Kromdraai B sample. 3). Analysis of different anatomical regions of the skull and the dentition may provide discordant results. For example, an assessment of overall cranial morphology points to possible microevolutionary processes in the *P. robustus* lineage (Martin et al., 2021), whereas a study of the bony labyrinth of specimens from the three sites found no evidence of morphological changes among the samples analyzed (Braga et al., 2021). 4). Taphonomic factors may have influenced composition in the fossil samples, that may not be representative of a natural population. In this regard, potential differences have been suggested between the Swartkrans and the DMQ samples (Riga et al., 2019), whereas little is known for the KB sample.

Among the newly described teeth, four permanent teeth have been attributed to the genus *Homo*. This brings the DMQ *Homo* permanent sample up to 12, adding to the relatively limited representation of fossils attributed to this genus in the Early Pleistocene of South Africa. The RM^1 specimens DNH 99 shows affinities with DNH 70, although smaller in MD and BL dimensions. It also lacks the marked MD elongation of M^1 specimens from Swartkrans such ad SK 27 and SKW 3114. The specimen DNH 100 (LM_2) has morphological traits also present in other lower molars attributed to South African *Homo*. In terms of size, the only two other measurable lower M2 of South African *Homo* are SK 15 and SK 45. DNH 100 shows similar degree of MD elongation. The developing crowns of the two teeth of DNH 102 (a LI_2 and a L_C) shows remarkable morphological affinities with the Swartkrans *Homo* specimen SKX 2354/2355/2356 where SKX is the developing crown of a LI_2 and SKX 2356 is the developing crown of a L_C.

6 | CONCLUSIONS

Since its discovery in 1992, the DMQ has become a rich source of hominin fossil material attributed to *P. robustus* and at least one *Homo* species. With over 150 fossil hominin specimens recovered so far DMQ provides, after Swartkrans, the largest sample of *P. robustus*. The DMQ hominin site-sample is dominated by craniodental specimens (*c*.90%). Most are dental, either isolated teeth or maxillary and mandibular specimens that include teeth (Herries et al., 2020; Keyser, 2000; Martin et al., 2021; Moggi-Cecchi et al., 2010). The benefit of the new evidence from DMQ is not limited to an increase in sample sizes for tooth types and positions represented at the other sites. It also provides evidence about teeth not present at either Swartkrans or Kromdraai B. Overall, the DMQ hominin collection is now the second largest sample of *P. robustus* after Swartkrans, and still outnumbers the recently expanded sample from Kromdraai B (Braga, Dumoncel, et al., 2016; Braga, Fourvel, et al., 2016).

Through the years, analysis of the craniodental remains has allowed several issues related to the paleobiology of *P. robustus*, such as taxonomy (Herries et al., 2020; Keyser et al., 2000; Martin et al., 2021; Moggi-Cecchi et al., 2010), taphonomic history (Riga et al., 2019), temporal frameworks (Herries et al., 2020), and microevolutionary trends (Martin et al., 2021), to be addressed. The new set of 24 teeth described here further expands the rich hominin sample recovered from DMQ and helps to elucidate specific points of *P. robustus* paleobiology. The recovery of a lower di1 (DNH 88) adds a new tooth class to the *P. robustus* sample from DMQ and adds to the only other lower di1 of *P. robustus* from Swartkrans (SK 61). The 7 new deciduous teeth and 7 new permanent developing teeth reinforces previous observations that the DMQ assemblage contains a higher percentage of subadult/juvenile specimens as compared to other deposits (Riga et al., 2019).

The expanded *P. robustus* dental sample allowed us to re-examine previous analysis of metrical differences in tooth size and patterns of variation among the two site-samples here considered (DMQ and Swartkrans). Although no clear-cut differences emerge when considering both the maxillary and mandibular dentitions, overall significant differences emerge in the mean values of both the MD and BL variables of the postcanine maxillary teeth between the two sites. These results show the Swartkrans *P. robustus* specimens tend to be larger in size than those at DMQ—consistent with the results of our previous analysis (Moggi-Cecchi et al., 2010). The pattern of differences presented here does not contradict the hypothesis of dental size increase in the *P. robustus* lineage (Martin et al., 2021) nor does it contradict the hypothesis of a sampling bias at the Swartkrans site (Riga et al., 2019). At the same time, we need to stress the fact that the average *n* value for all permanent dental classes in the DMQ assemblage is $n = 5$, with a range of 1 to 9, representing a limitation on this analysis and interpretations thereof. Any addition to the DMQ or the Swartkrans samples may alter this result. The analysis of variation within and between the two samples indicates a similar situation. Any conclusion based on the analysis of the metrical data of the permanent teeth alone should be then considered as preliminary, requiring further support by an expanded dental sample and by analysis of complementary set of morphological and metrical information gained from the dentition and other skeletal regions of the species *P. robustus*.

AUTHOR CONTRIBUTIONS

Angeline B. Leece: Formal analysis (lead); investigation (equal); methodology (equal); writing – original draft (lead); writing – review and editing (lead). **Jesse M. Martin:** Formal analysis (equal); investigation (equal); supervision (equal); writing – original draft (equal); writing – review and editing (equal). **Andy I. R. Herries:** Conceptualization (equal); funding acquisition (lead); project administration (lead); resources (lead); writing – review and editing (equal). **Alessandro Riga:** Formal analysis (equal); methodology (equal); resources (equal); software (equal); writing – original draft (equal). **Colin G. Menter:** Conceptualization (equal); funding acquisition (equal); investigation (equal); project administration (equal); resources (equal); supervision (equal). **Jacopo Moggi-Cecchi:** Conceptualization (lead); data curation (equal); formal analysis (equal); writing – original draft (lead); writing – review and editing (lead).

ACKNOWLEDGMENTS

Excavation that led to the recovery of the specimens presented here was partly funded by the Italian Ministry of Foreign Affairs – Archaeological Mission to South Africa to J.M.C. This research was

additionally funded by a research grant from an Australian Archaeological Association SRGS 2014 grant to A.B.L., an Australian Research Council Future Fellowship grant FT120100399 to A.I.R.H., two La Trobe University IRGS grants to A.B.L., a La Trobe University IRGS grant to J.M.M., and an ARC Discovery grant DP170100056 to A.I.R.H. Thanks to the student excavators of field schools run at the site by a combination of the University of Johannesburg, La Trobe University, Washington University in St. Louis, and the University of Victoria. Thanks to the former (D. and J. Smith) and current landowners (Nathi and Khethi Nkosi; Ngomo Lodge) and SAHRA for access to excavate at Drimolen. We would also like to thank Bernhard Zipfel (Evolutionary Studies Institute, University of the Witwatersrand) for facilitating access to the DMQ fossil specimens and to Stephanie Potze, Heidi Fourie, and Mirriam Tawane for facilitating access to the Swartkrans collections at the Ditsong National Museum of Natural History. Open Access Funding provided by Universita degli Studi di Firenze within the CRUI-CARE Agreement.

FUNDING INFORMATION

Italian Ministry of Foreign Affairs – Archaeological Mission to South Africa, Australian Archaeological Association SRGS 2014, Australian Research Council Future Fellowship grant FT120100399, La Trobe University IRGS, ARC Discovery grant DP170100056.

CONFLICT OF INTEREST

The authors declare no potential conflict of interest.

DATA AVAILABILITY STATEMENT

The data that support the findings of this study are available from the corresponding author upon reasonable request.

ORCID

Angeline B. Leece https://orcid.org/0000-0003-3348-3726
Jesse M. Martin https://orcid.org/0000-0002-6275-6079
Andy I. R. Herries https://orcid.org/0000-0002-2905-2002
Alessandro Riga https://orcid.org/0000-0002-7240-0009
Colin G. Menter https://orcid.org/0000-0003-1066-8496
Jacopo Moggi-Cecchi https://orcid.org/0000-0001-5055-8369

REFERENCES

Adams, J. W., Rovinsky, D. S., Herries, A. I. R., & Menter, C. G. (2016). Macromammalian faunas, biochronology and palaeoecology of the early Pleistocene Main Quarry hominin-bearing deposits of the Drimolen Palaeocave System, South Africa. *PeerJ*, *4*, 1941.

Balter, V., Blichert-Toft, J., Braga, J., Telouk, P., Thackeray, F., & Albarède, F. (2008). U–Pb dating of fossil enamel from the Swartkrans Pleistocene hominid site, South Africa. *Earth and Planetary Science Letters*, *267*(1–2), 236–246.

Blackwell, B. A. (1994). Problems associated with reworked teeth in electron spin resonance (ESR) dating. *Quaternary Science Reviews*, *13*(5–7), 651–660.

Braga, J., Dumoncel, J., Duployer, B., Tenailleau, C., de Beer, F., & Thackeray, J. F. (2016). The Kromdraai hominins revisited with an updated portray of differences between *Australopithecus africanus* and *Paranthropus robustus*. In J. Braga & J. F. Thackeray (Eds.), *Kromdraai, a birthplace of Paranthropus in the cradle of humankind*. Sun Media Metro.

Braga, J., Fourvel, J.-B., Lans, B., Bruxelles, L., & Thackeray, J. F. (2016). Evolutionary, chrono-cultural and palaeoenvironmental backgrounds to the Kromdraai site: A regional perspective. In J. Braga & J. F. Thackeray (Eds.), *Kromdraai, a birthplace of Paranthropus in the cradle of humankind*. Sun Media Metro.

Braga, J., Samir, C., Fradi, A., Feunteun, Y., Jakata, K., Zimmer, V. A., Zipfel, B., Thackeray, J. F., Macé, M., Wood, B. A., & Grine, F. E. (2021). Cochlear shape distinguishes Southern African early hominin taxa with unique auditory ecologies. *Scientific Reports*, *11*(1), 17018.

Braga, J., & Thackeray, F. (2003). Early *Homo* at Kromdraai B: Probabilistic and morphological analysis of the lower dentition. *Comptes Rendus Palevol*, *2*, 269–279.

Braga, J., Thackeray, J. F., Bruxelles, L., Dumoncel, J., & Fourvel, J.-B. (2017). Stretching the time span of hominin evolution at Kromdraai (Gauteng, South Africa): Recent discoveries. *Comptes Rendue Palevol*, *16*, 58–70.

Braga, J., Thackeray, J. F., Dumoncel, J., Descouens, D., Bruxelles, L., Loubes, J.-M., Kahn, J.-L., Stampanoni, M., Bam, L., Hoffman, J., de Beer, F., & Spoor, F. (2013). A new partial temporal bone of a juvenile hominin from the site of Kromdraai B (South Africa). *Journal of Human Evolution*, *65*(4), 447–456.

Brain, C. K. (1981). *The hunters of the hunted?: And introduction to African cave taphonomy*. University of Chicago Press.

Brain, C. K. (1993). *Swartkrans: A Cave's chronicle of early man* (p. 8). Transvaal Museum Monograph.

Brink, J., Herries, A. I. R., Moggi-Cecchi, J., Gowlett, J., Adams, J. W., Hancox, J., Bousman, C. B., Grün, R., Eisenmann, V., Adams, J. W., & Rossouw, L. (2012). First hominine remains from ~1 Ma bone bed at Cornelia-Uitzoek, Free State Province, South Africa. *Journal of Human Evolution*, *63*, 527–535.

Broom, R., & Robinson, J. T. (1952). Swartkrans ape-man, *Paranthropus crassidens*. *Transvaal Museum Monography*, *6*, 123.

Bruxelles, L., Maire, R., Couzens, R., Thackeray, J. F., & Braga, J. (2016). A revised stratigraphy of Kromdraai. In J. Braga & J. F. Thackeray (Eds.), *Kromdraai, a birthplace of Paranthropus in the cradle of humankind*. Sun Media Metro.

Clarke, R. J. (1977). A juvenile cranium and some adult teeth of early *Homo* from Swartkrans, Tranvsaal. *South African Journal of Science*, *73*, 46–49.

Clarke, R. J., Howell, F. C., & Brain, C. K. (1970). New finds at the Swartkrans australopithecine site (contd): More evidence of an advanced hominid at Swartkrans. *Nature*, *225*(5239), 1219–1222.

Curnoe, D., Grün, R., Taylor, L., & Thackeray, F. (2001). Direct ESR dating of a Pliocene hominin from Swartkrans. *Journal of Human Evolution*, *40*, 379–391.

Curnoe, D., Grün, R., & Thackeray, F. (2002). Electron spin resonance dating of tooth enamel from Kromdraai B, South Africa. *South African Journal of Science*, *98*, 540.

Donnelly, S. M., & Kramer, A. (1999). Testing for multiple species in fossil samples: An evaluation and comparison of tests for equal relative variation. *American Journal of Physical Anthropology*, *108*, 507–529.

Gibbon, R. J., Pickering, T. R., Sutton, M. B., Heaton, J. L., Kuman, K., Clarke, R. J., & Granger, D. E. (2014). Cosmogenic nuclide burial dating of hominin-bearing Pleistocene cave deposits at Swartkrans, South Africa. *Quaternary Geochronology*, *24*, 10–15.

Grine, F. E. (1984). *The deciduous dentition of the Kalahari San, the South African negro and the South African Plio-Pleistocene hominids*. University of the Witwatersrand.

Grine, F. E. (1985). Australopithecine evolution: The deciduous dental evidence. In E. Delson (Ed.), *Ancestors: The hard evidence* (pp. 153–167). Alan R. Liss.

Grine, F. E. (1988). New craniodental fossils of *Paranthropus* from the Swartkrans formation and their significance in "robust"

australopithecine evolution. In F. E. Grine (Ed.), *Evolutionary history of the 'robust' australopithecines* (pp. 223–243). Aldine de Gruyter.

Grine, F. E. (1989). New hominid fossils from the Swartkrans formation (1979-1986 excavations): Craniodental specimens. *American Journal of Physical Anthropology*, *79*, 409–449.

Grine, F. E. (2005). Early *homo* at Swartkrans, South Africa: A review of the evidence and an evaluation of recently proposed morphs. *South African Journal of Science*, *101*, 43–52.

Grine, F. E., Smith, H. F., Heesy, C. P., & Smith, E. J. (2009). Phenetic affinities of plio-pleistocene *Homo* fossils from South Africa: Molar cusp proportions. In F. E. Grine, J. G. Fleagle, & R. E. Leakey (Eds.), *The first humans—Origin and early evolution of the genus Homo. Vertebrate Paleobiology and Paleoanthropology* (pp. 49–62). Springer.

Grine, F. E., & Strait, D. S. (1994). New hominid fossils from Member 1 'Hanging Remnant.' Swartkrans Formation, South Africa. *Journal of Human Evolution*, *26*, 57–75.

Herries, A. I. R., & Adams, J. W. (2013). Clarifying the context, dating and age range of the Gondolin hominins and *Paranthropus* in South Africa. *Journal of Human Evolution*, *65*, 676–681.

Herries, A. I. R., Adams, J. W., Joannes-Boyau, R., Armstrong, B., Baker, S., Blackwood, A. F., Boschian, G., Caruana, M. V., Penzo-Kajewski, P., Murszewski, A., & Rovinsky, D. S. (2019). Integrating palaeocaves into palaeolandscapes: An analysis of cave levels and karstification history across the Gauteng Malmani dolomite, South Africa. *Quaternary Science Reviews*, *220*, 310–334.

Herries, A. I. R., Curnoe, D., & Adams, J. W. (2009). A multi-disciplinary seriation of early homo and Paranthropus bearing palaeocaves in southern Africa. *Quaternary International*, *202*(1–2), 14–28.

Herries, A. I. R., Martin, J. M., Leece, A. B., Adams, J. W., Boschian, G., Joannes-Boyau, R., Edwards, T. R., Mallett, T., Massey, J., Murszewski, A., Neubauer, S., Pickering, R., Strait, D. S., Armstrong, B. J., Baker, S., Caruana, M. V., Denham, T., Hellstrom, J., Moggi-Cecchi, J., … Menter, C. (2020). Contemporaneity of *Australopithecus*, *Paranthropus*, and early *Homo erectus* in South Africa. *Science*, *368*, 7293.

Herries, A. I. R., Murszewski, A., Pickering, R., Mallett, T., Joannes-Boyau, R., Armstrong, B., Adams, J. W., Baker, S., Blackwood, A. F., Penzo-Kajewski, P., & Kappen, P. (2018). Geoarchaeological and 3D visualisation approaches for contextualising in-situ fossil bearing palaeokarst in South Africa: A case study from the ~2.61 Ma Drimolen Makondo. *Quaternary International*, *483*, 90–110.

Herries, A. I. R., & Shaw, J. (2011). Palaeomagnetic analysis of the Sterkfontein palaeocave deposits; age implications for the hominin fossils and stone tool industries. *Journal of Human Evolution*, *60*, 523–539.

Howell, F. C. (1978). Hominidae. In J. V. Maglio & H. B. S. Cooke (Eds.), *Evolution of African mammals* (pp. 154–248). Harvard University Press.

Keyser, A. W. (2000). The Drimolen skull: The most complete australopithecine cranium and mandible to date. *South African Journal of Science*, *96*, 189–193.

Keyser, A. W., Menter, C. G., Moggi-Cecchi, J., Pickering, T. R., & Berger, L. R. (2000). Drimolen: A new hominid-bearing site in Gauteng, South Africa. *South African Journal of Science*, *96*, 193–197.

Kuman, K., & Clarke, R.J. (2000). Stratigraphy, artefact industries and hominid associations for Sterkfontein, Member 5. *Journal of Human Evolution*, *38*(6), 827–847.

Kuman, K., Granger, D. E., Gibbon, R. J., Pickering, T. R., Caruana, M. V., Bruxelles, L., Clarke, R. J., Heaton, J. L., Stratford, D., & Brain, C. K. (2021). A new absolute date from Swartkrans cave for the oldest occurrences of *Paranthropus robustus* and Oldowan stone tools in South Africa. *Journal of Human Evolution*, *156*, 103000.

Leece, A., Kegley, A. D. T., Lacruz, R. S., Herries, A. I. R., Hemingway, J., Kgasi, L., Potze, S., & Adams, J. W. (2016). The first hominin from the early Pleistocene paleocave of Haasgat, South Africa. *PeerJ*, *4*, e2024. https://doi.org/10.7717/peerj.2024

Martin, J. M., Leece, A. B., Neubauer, S., Baker, S. E., Mongle, C. S., Boschian, G., Schwartz, G. T., Smith, A. L., Ledogar, J. A., Strait, D. S., & Herries, A. I. R. (2021). Drimolen cranium DNH 155 documents microevolution in an early hominin species. *Nature Ecology & Evolution*, *5*(1), 38–45. https://doi.org/10.1038/s41559-020-01319-6

Menter, C. G., Kuykendall, K. L., Keyser, A. W., & Conroy, G. C. (1999). First record of hominid teeth from the Plio-Pleistocene site of Gondolin, South Africa. *Journal of Human Evolution*, *37*, 299–307.

Moggi-Cecchi, J., Menter, C. G., Boccone, S., & Keyser, A. (2010). Early hominin dental remains from the Plio-Pleistocene site of Drimolen, South Africa. *Journal of Human Evolution*, *58*, 374–405.

Murszewski, A., Boschian, G., & Herries, A. I. (2020). Complexities of assessing palaeocave stratigraphy: Reconstructing site formation of the ~2.61 Ma Drimolen Makondo fossil site. *PeerJ*, *8*, e10360.

Ngoloyi, N. M., Dumoncel, J., Thackeray, J. F., & Braga, J. (2020). A new method to evaluate 3D spatial patterns within early hominin-bearing sites. An example from Kromdraai (Gauteng Province, South Africa). *Journal of Archaeological Science Reports*, *32*, 102376.

Partridge, T. C. (1982). Some preliminary observations on the stratigraphy and sedimentology of the Kromdraai B hominid site. In J. A. Coetzee & E. M. van Zinderen Bakker (Eds.), *Palaeoecology of Africa and the surrounding islands* (Vol. 15, pp. 3–12). CRC Press, Taylor & Francis Group, New York.

Pickering, R., Herries, A. I. R., Woodhead, J. D., Hellstrom, J. D., Green, H. E., Paul, B., Ritzman, T., Strait, D. S., Schoville, B. J., & Hancox, P. J. (2019). South African hominin record restricted to dry phases as demonstrated by U-Pb dated flowstones. *Nature*, *565*, 226–229.

Pickering, T. R., Heaton, J. L., Clarke, R. J., Sutton, M. B., Brain, C. K., & Kuman, K. (2012). New hominid fossils from member 1 of the Swartkrans formation, South Africa. *Journal of Human Evolution*, *62*, 618–628.

Pickering, T. R., Heaton, J. L., Sutton, M. B., Clarke, R. J., Kuman, K., Senjem, J. H., & Brain, C. K. (2016). New early Pleistocene hominin teeth from the Swartkrans formation, South Africa. *Journal of Human Evolution*, *100*, 1–15.

R Core Team. (2017). *R: A language and environment for statistical computing*. R Foundation for Statistical Computing. https://www.R-project.org/

Rak, Y., Kimbel, W. H., Moggi-Cecchi, J., Lockwood, C. A., & Menter, C. (2021). The DNH 7 skull of Australopithecus robustus from Drimolen (Main quarry), South Africa. *Journal of Human Evolution*, *151*, 102913. https://doi.org/10.1016/j.jhevol.2020.102913

Reynolds, S. C., Clarke, R. J., & Kuman, K. (2007). The view from the Lincoln cave: Mid- to late Pleistocene fossil deposits from Sterkfontein hominid site, South Africa. *Journal of Human Evolution*, *53*, 260–271.

Riga, A., Mori, T., Pickering, T. R., Moggi-Cecchi, J., & Menter, C. G. (2019). Ages-at-death distribution of the early Pleistocene hominin fossil assemblage from Drimolen (South Africa). *American Journal of Physical Anthropology*, *168*, 632–636.

Robinson, J.T. (1953). Telanthropus and its phylogenetic significance. *American Journal of Physical Anthropology*, *11*, 445–501.

Robinson, J. T. (1956). The dentition of the Australopithecinae. *Transvaal Museum Mem*, *9*, 1–179.

Rovinsky, D. S., Herries, A. I. R., Menter, C. G., & Adams, J. W. (2015). First description of in situ primate and faunal remains from the Plio-Pleistocene Drimolen Makondo palaeocave infill, Gauteng: South Africa. *Palaeontologia Electronica*, *2*, 1–21.

Schultz, B. (1985). Levene's test for relative variation. *Systematic Zoology*, *34*, 449–456.

Schwartz, J. H., & Tattersall, I. (2005). The human fossil record. In *Craniodental morphology of early hominids (Genera Australopithecus, Paranthropus, Orrorin and Overview)* (Vol. 4). Wiley-Liss.

Sokal, R. R., & Braumann, C. A. (1980). Significance tests for coefficients of variation and variability profiles. *Systematic Zoology*, *29*, 50–66.

Stratford, D., Heaton, J. L., Pickering, T. R., Caruana, M. V., & Shadrach, K. (2016). First hominin fossils from Milner Hall, Sterkfontein, South Africa. *Journal of Human Evolution*, *91*, 167–173.

Sutton, M. B., Pickering, T. R., Pickering, R., Brain, C. K., Clarke, R. J., Heaton, J. L., & Kuman, K. (2009). Newly discovered fossil- and artifact-bearing deposits, uranium-series ages and Plio-Pleistocene hominids at Swartkrans Cave, South Africa. *Journal of Human Evolution*, *57*, 688–696.

Thackeray, J. F., Kirschvink, J. L., & Raub, T. D. (2002). Palaeomagnetic analyses of calcified deposits from the Plio-Pleistocene hominid site of Kromdraai, South Africa: News & views. *South African Journal of Science*, *98*(11–12), 537–540.

Tobias, P. V. (1965). Australopithecus, Homo habilis, tool-using, and tool-making. *South African Archaeological Bulletin*, *20*, 167–192.

Tobias, P. V. (1967). Olduvai Gorge. In *The cranium and maxillary dentition of Australopithecus (Zinjanthropus) boisei* (Vol. II). Cambridge University Press.

Tobias, P. V. (1991). Olduvai Gorge. In *The skulls, endocasts and teeth of Homo habilis* (Vol. IV). Cambridge University Press.

Zanolli, C., Pan, L., Skinner, M., Dumoncel, J., Beaudet, A., de Beer, F., Hoffman, J., Jakata, K., Macchiarelli, R., Reddy, S., Tawane, M., & Zipfel, B. (2018). What is South African early *Homo*? New insights from the molar endostructural signature. *Proceedings of the European Society for Human Evolution*, *7*, 206.

SUPPORTING INFORMATION

Additional supporting information can be found online in the Supporting Information section at the end of this article.

How to cite this article: Leece, A. B., Martin, J. M., Herries, A. I. R., Riga, A., Menter, C. G., & Moggi-Cecchi, J. (2022). New hominin dental remains from the Drimolen Main Quarry, South Africa (1999–2008). *American Journal of Biological Anthropology*, 1–21. https://doi.org/10.1002/ajpa.24570